GEOSPHERE

GEOSPHERE; v. 14, no. 4

https://doi.org/10.1130/GES01545.1

9 figures; 1 table; 1 set of supplemental files

CORRESPONDENCE:
jean-noel.proust@univ-rennes1.fr

CITATION: Proust, J.-N., Pouderoux, H., Ando, H., Hesselbo, S.P., Hodgson, D.M., Lofi, J., Rabineau, M., and Sugarman, P.J., 2018, Facies architecture of Miocene subaqueous clinothems of the New Jersey passive margin: Results from IODP-ICDP Expedition 313: Geosphere, v. 14, no. 4, https://doi.org/10.1130/GES01545.1.

Science Editor: Shanaka de Silva
Guest Associate Editor: David Burns McInroy

Received 14 April 2017
Revision received 28 December 2017
Accepted 2 May 2018

Facies architecture of Miocene subaqueous clinothems of the New Jersey passive margin: Results from IODP-ICDP Expedition 313

Jean-Noël Proust[1,*], Hugo Pouderoux[1,*], Hisao Ando[2,*], Stephen P. Hesselbo[3,*], David M. Hodgson[4,*], Johanna Lofi[5,*], Marina Rabineau[6,*], and Peter J. Sugarman[7,*]

[1]Geosciences, CNRS, University of Rennes, Rennes 35042, France
[2]Department of Earth Science, College of Science, Ibaraki University, Bunkyo Mito 310-8512, Japan
[3]Camborne School of Mines, University of Exeter, Penryn Campus, Penryn, Cornwall TR10 9FE, UK
[4]School of Earth and Environment, University of Leeds, Leeds LS2 9JT, UK
[5]Géosciences, CNRS, University of Montpellier, Montpellier 34090, France
[6]Géosciences Océan, CNRS, Institut Universitaire Européen de La Mer, Plouzané 29280, France
[7]New Jersey Geological Survey, Trenton, New Jersey 08638, USA

ABSTRACT

Understanding the history, causes, and impact of sea-level changes is a challenge for our societies that face accelerated global sea-level rise. In this context, improvement of our knowledge of sea-level changes and shoreline migration at geological time scales is critical. The preserved, laterally correlative sedimentary record of continental erosion on passive margins has been used to reconstruct past sea level. However, the detailed nature of a basic clinothem progradational pattern observed on many of these margins is still poorly known. This paper describes the sedimentary facies and interprets the depositional environments and the architecture of the clinothems of the New Jersey shelf (offshore northeastern USA) to depict the origin and controls of the distribution of the sediment on the margin. We analyze 612 cores totaling 1311 m in length collected at three sites 60 km offshore Atlantic City, New Jersey, during International Ocean Discovery Program–International Continental Scientific Drilling Program (IODP-ICDP) Expedition 313. The three sites sampled the lower to middle Miocene passive margin sediments of the New Jersey shelf clinothems. We also collected wireline logs at the three sites and tied the sedimentary architecture to the geometry observed on seismic profiles. The observed sediment distribution in the clinoform complex differs from that of current models based on seismic data, which predict a progressive increase in mud and decrease in sand contents in a seaward direction. In contrast, we observe that the clinoforms are largely composed of muds, with sands and coarser material concentrated at the rollover, the bottomset, and the toe of the slope. The shelf clinothem topsets are storm-influenced mud whereas the foreset slope is composed of a mud wedge largely dominated by density current deposits (e.g., low-density turbidites and debrites). The architecture of the clinothem complex includes a composite stack of ~30-m-thick clinothem units each made up of four systems tracts (Transgressive, Highstand, Forced-Regressive, and Lowstand Systems Tract) building individual transgressive-regressive sequences. The presence of mud-rich facies deposited during highstands on the topset of the clinoform, 40–60 km offshore from the sand-prone shoreface deposit (observed in the New Jersey onshore delta plain), and the lack of subaerial erosion (and continental depositional environments) point to a depositional model involving a subaerial delta (onshore) feeding a distant subaqueous delta. During forced regressions, shelf-edge deltas periodically overstep the stacks of flood-influenced, offshore-marine mud wedges of the New Jersey subaqueous delta, bringing sand to the rollover and building up the large-scale shelf-prism clinothems. The clinothem complex develops on a gently dipping platform with a ramp-like morphology (apparent dip of 0.75°–0.5°) below mean storm wave base, in 30–50 m of water depth, 40–60 km seaward of the coastal area. Its shape depends on the balance between accommodation and sedimentation rates. Subaqueous deltas show higher accumulation rates than their subaerial counterparts and prograde three times further and faster than their contemporaneous shoreline. The increase in the intensity of waves (height and recurrence intervals) favors the separation between subaqueous and subaerial deltas, and as a consequence, the formation of a flat topset geometry, a decrease in flood events and fluvial discharge, an overall progressive decrease in sediment grain size (from sequence m5.45, ca. 17.8–17.7 Ma, onwards), as well as an increase in sedimentation rates on the foresets of the clinoforms. All of these are recognized as preliminary signals that might characterize the entry into the Neogene icehouse world.

INTRODUCTION

Passive margin successions are commonly characterized as relatively simple suites of sedimentary strata truncated by unconformities that can be correlated regionally, and in some cases worldwide. They show a gradational evolution of depositional environments from continental to deep marine realms,

*E-mail: jean-noel.proust@univ-rennes1.fr; hugo.pouderoux@univ-rennes1.fr; hisao.ando.sci@vc.ibaraki.ac.jp; s.p.hesselbo@exeter.ac.uk; d.hodgson@leeds.ac.uk; johanna.lofi@gm.univ-montp2.fr; marina.rabineau@univ-brest.fr; Pete.Sugarman@dep.state.nj.us

including the shoreline, and a well-known subsidence history. As such, passive margins have for a long time been used to reconstruct global sea-level variations on geological time scales (e.g., Vail et al., 1977; Miller et al., 2005). Sequence stratigraphy proved to be an effective tool to decipher the passive margin sedimentary record from the earliest outcomes of seismic stratigraphy (Vail et al., 1977; Posamentier et al., 1988) to the most recent standardization (e.g., Catuneanu et al., 2009), applications (e.g., Embry, 2009), and simplifications (Neal and Abreu, 2009; Miller et al., 2018). Numerous hypotheses, however, have not been fully tested yet, e.g., the nature of the sedimentary facies that compose the prograding clinothems on the shelf—a classic end member of most passive margin sedimentary records (e.g., Mitchum et al., 1977; Berg, 1982; Alexander et al., 1991; Pirmez et al., 1998; Hubbard et al., 2010, Helland-Hansen et al., 2012). Similarly, the timing and phase relationship of these sedimentary facies with respect to relative sea-level changes (Reynolds et al., 1991) or the paleo–water depth of sediment deposited at the top and the toe of the clinoforms (Greenlee and Moore, 1988) have not been determined definitively. Clinoforms are distinct sigmoidal geometric features associated with topset, foreset, and bottomset deposits that generally prograde seaward (termed a clinothem). Clinothem topsets were originally termed as the shelf and the rollover point at the shelf break (Vail et al., 1977). This has created confusion because the modern continental shelf-slope break is typically in 120–200 m of water (e.g., Heezen et al., 1959), and it has been shown that the rollover features (also called "depositional shelf breaks") associated with clinothems are shallower, showing different features than the shelf-slope break.

This paper seeks to ground-truth the vertical succession and lateral facies associations of clinothems in the relatively simple passive margin system of the New Jersey shelf (offshore northeastern USA) by using the data provided by International Ocean Discovery Project–International Continental Scientific Drilling Program (IODP-ICDP) Expedition 313 (Mountain et al., 2010a, 2010b). We examine successively the sedimentary facies found in the coreholes, and the seismic and sedimentary architecture of the clinothems; we propose a stratigraphic and depositional model for the New Jersey clinothems that combines subaerial-subaqueous delta with shelf prism–scale clinoforms and discuss some important factors controlling this complex architecture.

BACKGROUND WORK

The New Jersey shelf is part of the U.S. mid-Atlantic margin that extends from New Jersey through Delaware to Maryland (Fig. 1). The U.S. Atlantic margin is a classic passive margin, which showed a rifting phase in the Late Triassic (ca. 230–198 Ma; Sheridan and Grow, 1988; Withjack et al., 1998) and seafloor spreading commencing during the Early to Middle Jurassic (180–165 Ma), followed by thermal subsidence, sediment loading, and flexure (Watts and Steckler, 1979; Reynolds et al., 1991). The sedimentary succession consists of Upper Triassic alluvial, evaporitic, and restricted marine sediments injected by dikes, sills, and lava flows, overlain by a thick (8–12 km) Jurassic to mid-Cretaceous limestone and shale succession fringed by a barrier reef complex (Poag, 1985a). Sedimentation rates decreased from the Late Cretaceous to the Paleogene, building up a mixed siliciclastic carbonate ramp ending in a condensed and starved clay-rich carbonate ramp with the general cooling of temperatures, by the late middle Eocene (onshore) to earliest Oligocene (offshore) (Miller and Snyder, 1997; Steckler et al., 1999). Due to the increase of tectonically and/or climatically driven denudation in the hinterland (Poag and Sevon, 1989; Poag, 1992; Poag and Ward, 1993), sediment supply increased in the late Oligocene and Miocene, building out progressively a large set of prograding clinothems (Fulthorpe and Austin, 1998) that were capped by Pleistocene deposits (Davies et al., 1992; Austin et al., 1995, 1996).

The New Jersey shelf prograding clinothems were first recognized with (low-resolution) multi-channel seismic profiles collected by Grow et al. (1979) and Schlee (1981) to image rift-stage sediments. Later studies outlined Paleogene and Neogene sequences (e.g., Poag and Schlee, 1984; Poag, 1985b; Poag and Ward, 1987; Greenlee and Moore, 1988) and, by using higher-resolution seismic data (from cruise Ew9009 [http://www-udc.ig.utexas.edu/sdc/cruise.php?cruiseln=ew9009] on the R/V *Ewing* in 1990, cruise Oc270 [http://www-udc.ig.utexas.edu/sdc/cruise.php?cruiseln=oc270] on the R/V *Oceanus* in 1995, and cruise CH0698 [http://www-udc.ig.utexas.edu/sdc/cruise.php?cruiseln=ch0698] on the R/V *Cape Hatteras* in 1998; Fig. 1), the three-dimensional (3-D) geometry and lateral variability of the Miocene depocenters (Fulthorpe and Austin, 1998; Fulthorpe et al., 1999; Poulsen et al., 1998; Monteverde et al., 2008) tied to the available industry and Ocean Drilling Program (ODP) coreholes drilled on the coastal plain (Legs 174AX and 150X) and on the outer shelf and slope (Legs 174A and 150) (Fig. 2A).

These studies have provided the chronology of sedimentation on the New Jersey shelf for the last 100 m.y. (e.g., Poag, 1985b; Miller et al., 1998, 2005; Browning et al., 2006, 2013). The sequence boundaries recognized onshore from facies successions are correlated to the continental slope with a ±0.5 m.y. accuracy and tied to the glacio-eustatic lowerings associated with $\delta^{18}O$ increases (Miller et al., 1998). The timing and the number of Miocene sequences fit with the Bahamas carbonate sequences (ODP Leg 166; Eberli et al., 1997) and the published Exxon Production Research global sea-level curve (Vail et al., 1977; Haq et al., 1987), although they significantly differ in amplitudes and rates (Van Sickel et al., 2004; Miller et al., 2005).

Despite the real progress presented by these studies, coastal plain cores missed most of the lowstand deposits due to changes in sea level of low to intermediate amplitudes that induce large unconformities and hiatuses, while the coreholes from the shelf edge and slope either failed to sample the sandy intervals (ODP Leg 174A) or provided a muddy homogeneous facies succession (ODP Leg 150), forming a poor basis for detailed inference of sea-level changes (Fig. 2). The IODP-ICDP Expedition 313 was specifically designed to fill this gap of knowledge and complement the New Jersey U.S. margin transect by drilling three holes in an intermediate position in the inner part of the New Jersey shelf in order to (1) recover most of the early to mid-Miocene interval in sea-level history including that inferred from the

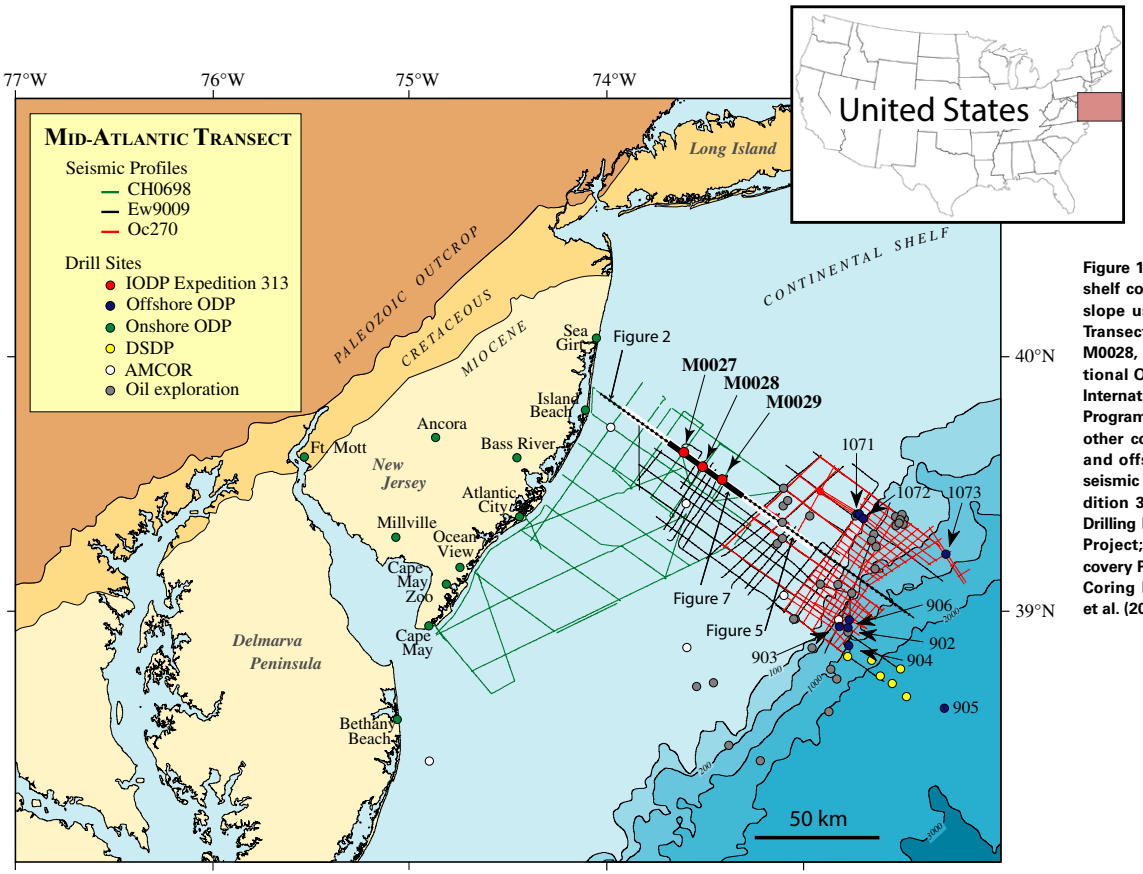

Figure 1. Location map of the New Jersey shelf coring sites on land, mid-shelf, and slope used to build up the Mid-Atlantic Transect. The figure shows Holes M0027, M0028, and M0029 drilled during International Ocean Discovery Program (IODP)–International Continental Scientific Drilling Program (ICDP) Expedition 313 along with other completed boreholes both onshore and offshore. Tracks of reconnaissance seismic lines relevant to the goals of Expedition 313 are also shown. ODP—Ocean Drilling Program; DSDP—Deep Sea Drilling Project; IODP—International Ocean Discovery Program; AMCOR—Atlantic Margin Coring Project. Modified from Mountain et al. (2010b) and Kominz et al. (2016).

lowstand deposits and (2) provide a large and diversified set of sedimentary facies very sensitive to changes in sea level (Mountain et al., 2009) that can be easily interpreted in terms of paleo–water depths. Three holes were drilled in the inner shelf targeting the upper Oligocene to middle Miocene seismically imaged prograding clinothems (Fig. 2B). The three holes drilled in 34–36 m of water, 45–67 km offshore, sample a 22-km-long clinothem transect including the topset, foreset, and toeset of several clinothems from 180 to 750 m below seafloor (mbsf).

Building on seismic stratigraphy of Monteverde et al. (2008), Expedition 313 drilled through 25 regionally mapped Oligocene to Miocene seismic surfaces that correlate to facies changes in the coreholes (Mountain et al., 2010; Inwood et al., 2013; Miller et al., 2013a, 2013b; Browning et al., 2013). The lithostratigraphic description of split cores shows silt-rich supply systems that reveal a notable depletion in clays and a marked difference between the top and the toe of the clinoform bodies (e.g., Lofi et al., 2013). The topset facies succession shows well-sorted silts and sands deposited in offshore to shoreface, mixed wave- to river-dominated shelf environments. The toe of the clinothems show silts and silty clays deposited below wave base. These sediments are typically interbedded with poorly sorted silts and sands deposited by continuous downslope gravity transport processes such as debris flows and turbidity currents during periods of clinoform rollover and upper slope degradation (Hodgson et al., 2018). The open shelf experienced frequent cycles of dysoxia. In situ and reworked glauconite is a common component of topset and bottomset strata that also show sharp changes in pore water salinity. Strontium isotopic ages measured on molluscs and foraminifers, reliable biostratigraphic zonation of multiple fossil groups (foraminifers, dinocysts and nannofossils; Katz et al., 2013; Browning et al., 2013), and specific pollen markers (McCarthy et al., 2013; Kotthoff et al., 2014) verify a nearly continuous

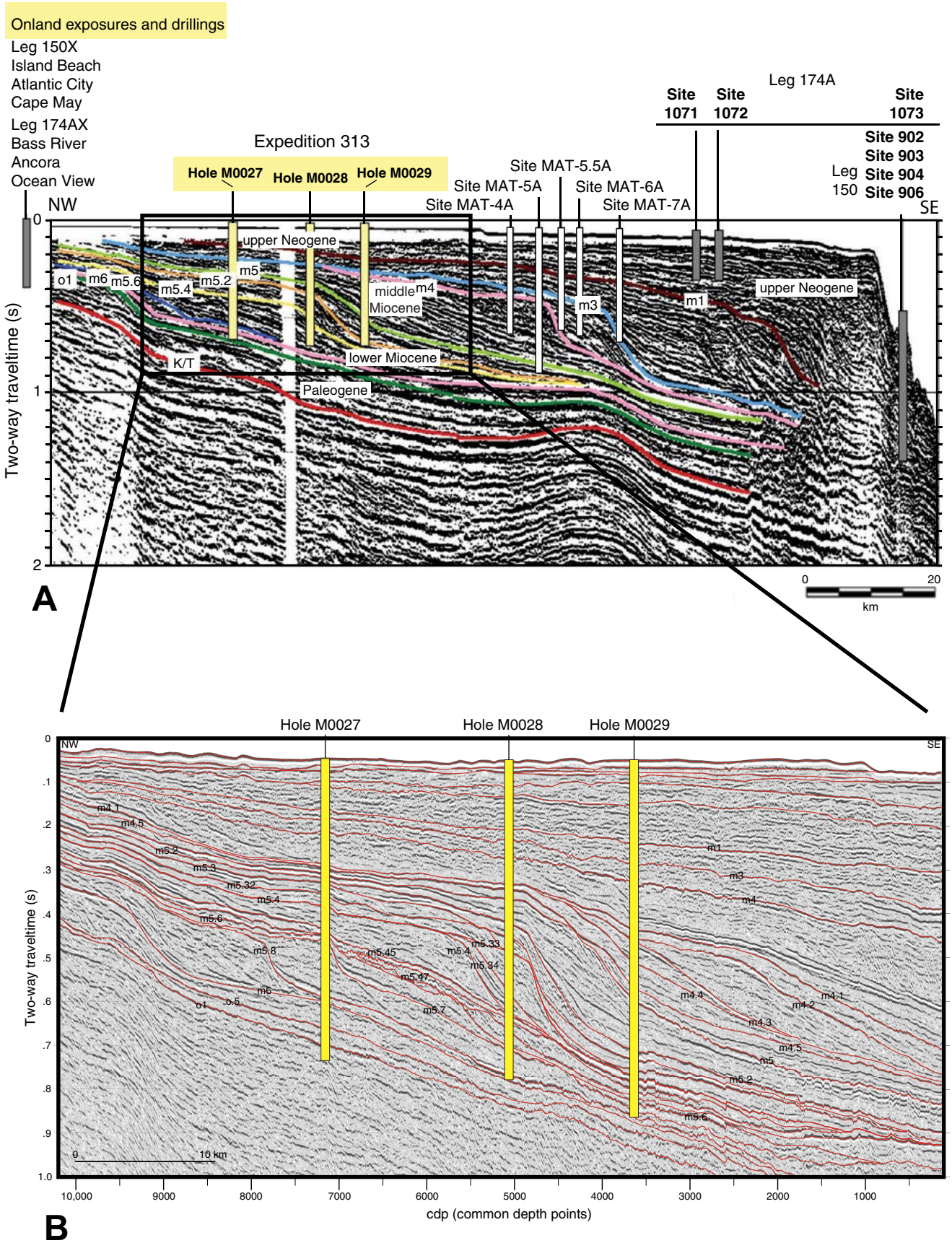

Figure 2. Drillhole locations projected on a regional seismic line through the New Jersey shelf. (A) R/V *Ewing* cruise Ew9009 seismic line 1003 through Holes M0027, M0028, and M0029 (yellow subseafloor columns; see Fig. 1 for location). Generalized locations of Ocean Drilling Program boreholes onshore and offshore (gray columns) and alternate sites also suitable for clinothem sampling in deeper waters (sites MAT-4A to MAT-7A, white columns) are also shown. The main key surfaces (colored lines; Cretaceous–Paleogene [Cretaceous–Tertiary, K/T] boundary = ca. 65 Ma, o1 = ca. 33.5 Ma, m5 = ca. 16.5 Ma, m4 = ca. 14 Ma, m3 = ca. 13.5 Ma, and m1 = ca. 11.5 Ma) have been traced from the inner shelf to the slope. The clinoform shape of sediments bracketed by these unconformities is thought to be the result of large sea-level fluctuations (Vail and Mitchum, 1977). (B) R/V *Oceanus* cruise Oc270 seismic line 529 with superposed seismic sequence boundaries interpreted by Monteverde et al. (2008) and drill depths at each of the three Expedition 313 sites (M0027, M0028, and M0029).

record of ~1 m.y. sea-level cycles and climate variations that may explain facies changes along the slopes of the clinoforms. We found no evidence of sea-level drop below the clinoform inflection point—i.e., depositional shelf break or offlap break—but the occurrence of shoreface deposits along the slope of the clinoforms and of deep water facies on their topsets suggest large changes in amplitude of relative sea level in the range of 60 m (Mountain et al., 2010a, 2010b).

DATA AND METHOD

Despite the difficulties of coring the sandy material of the shallow New Jersey shelf, 612 cores were collected at three sites (Sites M0027, M0028, and M0029) with 80% recovery for a total of 1311 m (Mountain et al., 2010a, 2010b). The deepest hole (M0029A) reached 757 mbsf; the oldest sediment (uppermost Eocene) was recovered in Hole M0027A. Besides the cores, the expedition collected wireline logs at the three sites—gamma ray, resistivity, magnetic susceptibility, sonic, acoustic televiewer, and vertical seismic profiles—which, together with multisensor core logs on unsplit cores, provide precise ties between core logs and seismic profiles (Mountain et al., 2010a, 2010b; Miller et al., 2013b). This data set was complemented post-cruise by the shipboard party by visual core descriptions and smear slide analyses, biostratigraphy (calcareous nannoplankton, diatoms, dinoflagellate cysts), magnetostratigraphy, and pore water geochemistry; paleobathymetry and paleoenvironments inferred from benthic foraminifera assemblages, dinocysts, pollen analyses, and grain size analysis (Ando et al., 2014). Multi-sensor core logger (MSCL) and petrophysical data were directly measured on cores and core sections (Inwood et al., 2013); Sr analyses were performed as an aid to get additional age control on the sediment and to evaluate the length of time represented by key stratal surfaces (Miller et al., 2013b; Browning et al., 2013).

Here we present a detailed analysis of the lithofacies successions and their interpretation in terms of depositional environment based on visual core description. Genetically related facies successions are bounded by unconformities tied to the interpreted seismic line 529 (cruise Oc270) (Monteverde et al., 2008) crossing the three holes, by using MSCL and downhole (impedance) log data (Miller et al., 2013b). In the following, we use the updated version of the stratal ages of Mountain et al. (2010b) provided by Browning et al. (2013).

RESULTS

The most striking feature of the early to mid-Miocene sediments of the New Jersey passive margin, as seen on the seismic line 529 of cruise Oc270, is the clinoform shape of the reflectors (Fig. 2). Here we present a description of the main lithofacies of the clinothems sampled in Site M0027, M0028, and M0029 coreholes of Expedition 313 and an interpretation of their depositional environments (Fig. 3; Supplemental Files [Figs. S1–S3][1]). Based on the established ties between the cores and the Oc529 seismic line (Mountain et al., 2010b; Miller et al., 2013a, 2013b), we reconstruct the lateral facies distribution along a two-dimensional (2-D) dip-oriented line across the margin, and interpret their depositional environments, systems tracts, and sequences.

Lithofacies and Depositional Environments

The lithofacies observed in cores are described below from the deep offshore marine to the shallow marine shoreface environments (Table 1). Numbers in the text refer to the hole and the lithofacies label (e.g., 27-1 refers to Hole M0027 and lithofacies 1; 28-4 refers to Hole M0028 and lithofacies 4; etc.) shown in Figure 3 and with more details in the Supplemental Files (Figs. S1–S3 [footnote 1]).

Offshore Marine Gravity-Flow Deposits—Lithofacies Association 1 (FA1)

Gravity flow deposits are abundant at the base of the three holes (M0027, 480–625 m; M0028, 500–610 m; M0029, 600–730 m; Fig. 3) and in the middle part of Hole M0029 (450–500 m; Fig. 3). Their lithological diversity is very large. They are here tentatively grouped in two broad categories, but a detailed description of their occurrence along the bottomsets of the clinothems can be found in Hodgson et al. (2018).

Amalgamated toe-of-slope debrites and turbidites—FA1.1. Lithofacies association FA1.1 occurs above seismic surfaces at the bottomset of clinoforms (Fig. 3). The lithofacies comprises a few-meters-thick, poorly sorted, glauconitic and quartzitic, medium to coarse sand with angular quartz granules and gravels, clay clasts, and, in places, a muddy matrix. Glauconite content can decrease upsection from 80%–90% (lithofacies 27-4, 28-6) to <40% (28-7), or to 5% with increasing mud content and decreasing quartz grain concentration (29-15). At the base, the facies is homogeneous and well bedded (27-4, 27-5, 28-6, 28-2), alternating with pale brown clay beds with nannofossils, locally cemented by carbonates and bioturbated by clay-lined horizontal and vertical burrows filled by glauconite (up to 87 cm below erosion surfaces). The gravel to medium sand beds show crude normal and reverse grading, with 1-m-high oblique stratification (15° apparent dip) underlined by muddy lamina cut by clay-filled *Chondrites* trace fossils (27-5, 28-6) and ripple and low-angle lamination. Upsection, the facies thins and fines upward (rarely coarsening), organized in meter-scale successions (28-7, 27-6, 28-9, 29-9, 29-13, 29-15, 29-18) capped by bioturbated horizons. Parallel and ripple cross-lamination give rise to finer-grained sediment with faint low-energy horizontal lamination, convolution, and laminae with a chaotic pattern. Thick- and thin-walled shell fragments are scattered throughout but show signs of severe dissolution. Locally, concretions and quartz granules have a patchy green coating or shattered fabric (e.g., 29-15). No plant debris or mica is observed.

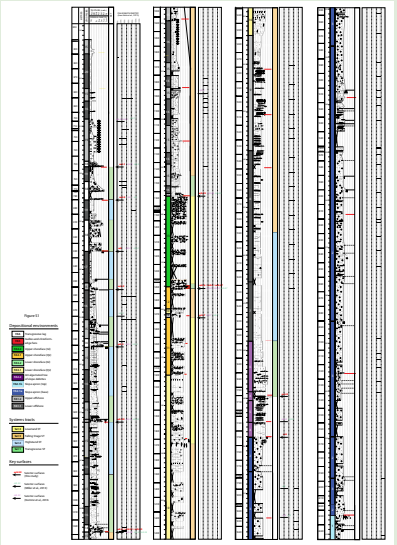

[1]Supplemental Files. Figure S1 is detailed lithological sections of hole M0027 drawn from the visual core descriptions. Figure S2 is detailed lithological sections of hole M0028 drawn from the visual core descriptions. Figure S3 is detailed lithological sections of hole M0029 drawn from the visual core descriptions. Please visit https://doi.org/10.1130/GES01545.S1 or the full-text article on www.gsapubs.org to view the Supplemental Files.

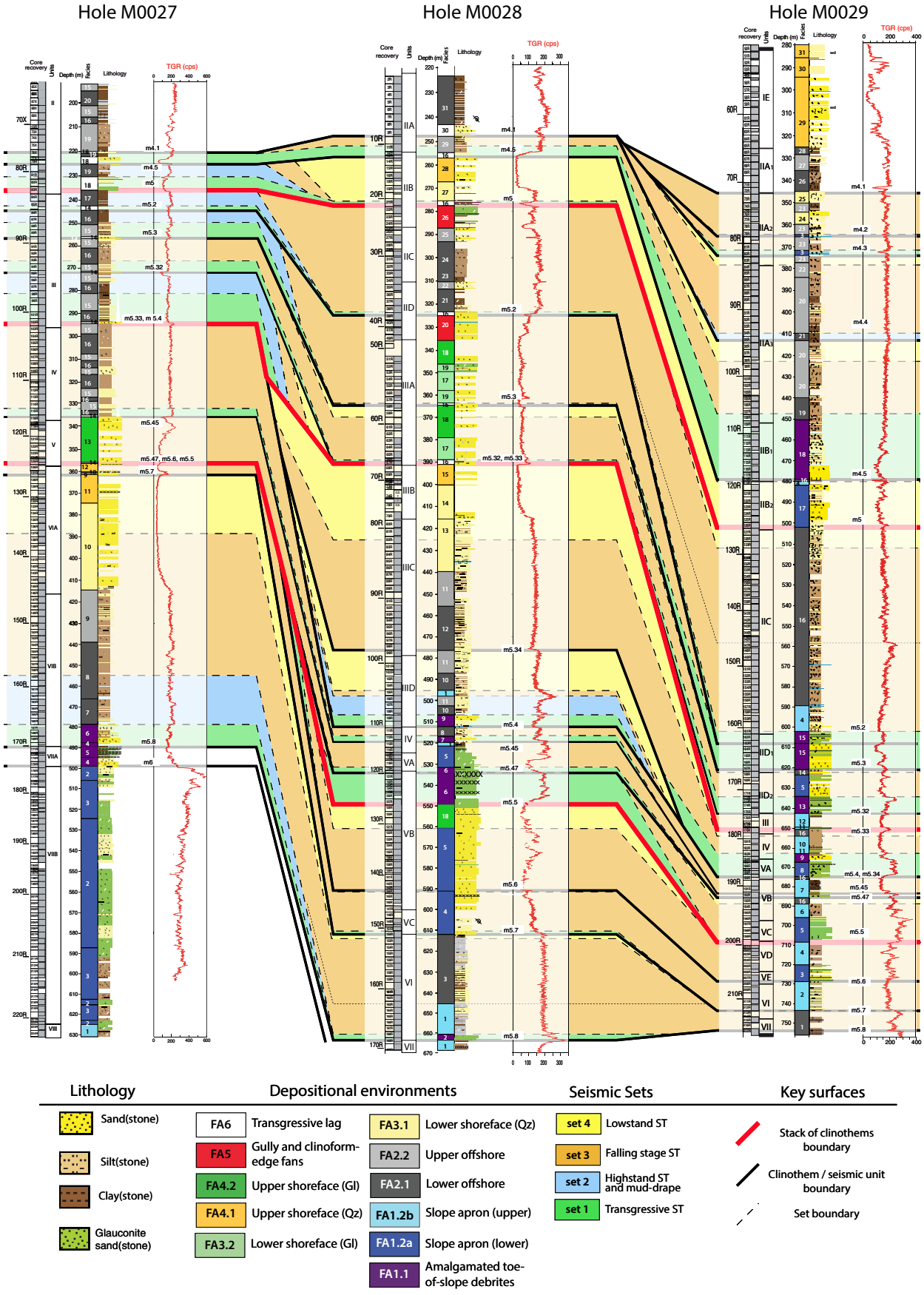

Figure 3. Simplified lithologic columns of the three Expedition 313 Holes M0027, M0028, and M0029 with the downhole total gamma ray log (TGR; cps—count per second); the inferred location on cores of the seismic unconformities (m4.1 to m6) observed on R/V *Oceanus* cruise Oc270 seismic line 529, based, with minor changes, on previous works of Mountain et al. (2010b), Miller et al. (2013a, 2013b), and Browning et al. (2013); and interpreted depositional environments and systems tracts (STs). A simplified description of the lithofacies, annotated with the number shown in colored boxes for each hole (e.g., "27-1" is lithofacies 1 in Hole M0027, "28-4" is lithofacies 4 in Hole M0028, etc.), can be found in Table 1 and in the detailed sections in the Supplemental Files (Figs. S1, S2, and S3; footnote 1). Numbers referred to in the core recovery columns are the core section numbers. The grey areas next to the core section numbers show the importance of the sediment recovery in each section. The location of the sediment gaps is unknown, so core recovery is arbitrarily affected in depth to the top of each section. Gl—glauconite, Qz—quartz.

TABLE 1. SUMMARY OF THE MAIN LITHOFACIES AND LITHOFACIES ASSOCIATIONS RECOGNIZED IN HOLES M0027, M0028, AND M0029 ON THE NEW JERSEY SHELF, WITH THEIR DEPOSITIONAL ENVIRONMENT INTERPRETATIONS

Lithofacies association			Lithofacies			Lithology			Sedimentary structures	Glauconite content	Bioturbation	Observations	Comments
			M0027	M0028	M0029	Grain size	Sorting	Grading					
FA1—Offshore marine gravity flow deposits	FA1.1—Amalgamated toe of slope debrites		27-4; 27-5; 27-6	28-2; 28-6; 28-7; 28-9	29-9; 29-13; 29-15; 29-18	Medium to coarse sand	Poor	Variable; usually normal	Well stratified; massive to oblique stratification; ripple and low-angle laminations; parallel and ripple cross-laminations; convolute lamination	Abundant	Moderate; presence of glauconite-filled burrows	Angular quartz granules and gravels; clay clasts; muddy matrix locally; clay beds with nannofossils; thick- and thin-walled shell fragments with sign of severe dissolution; quartz granules and concretions may have a patchy green coating; no plant debris or mica	**Healing phase**
	FA1.2—Slope apron deposits	FA1.2a	27-2; 27-3	28-4; 28-5	29-3; 29-5; 29-8; 29-17	Muddy medium to coarse sand with centimeter-thick clay beds	Poor	Variable; reverse and normal	Generally massive; subhorizontal laminations; ripple laminations; contorted and convolute laminations	Abundant; mix of mature and immature grains	Locally strong; underlines basal erosional contact	Dispersed granules; local concentration of pebbles; possible basal lag of granules; mud-supported granule and pebble sands within clay beds; variable amount of shell fragments, benthic foraminifers, wood and plant debris, and mica flakes; local presence of articulated shells and well-preserved benthic foraminifers	**Lower fan**
		FA1.2b	27-1	28-1	29-1; 29-4; 29-6; 29-7; 29-10; 29-11; 29-12	Fine to medium sand to silty clay	Good	Normal	Rare ripple-scale cross-laminations; remnant of planar laminations	Abundant; mix of mature and immature grains	Moderate; presence of glauconite-filled burrows	Floating coarse and very coarse quartz sand and glauconite grains; foraminifers; thin-walled shell fragments; thick-walled shell fragments with sign of severe dissolution; traces of plant debris and mica	**Upper fan**
FA2—Storm- and river-influenced offshore marine deposits	FA2.1—Lower offshore deposits	FA2.1a	27-7; 27-8	28-3; 28-10; 28-12	29-2	Clayey silt to very fine sand	Good	Reverse	Poorly laminated to ripple cross-laminations and low-angle to planar horizontal laminations	Trace; mostly in burrow infills	Weak	Nannofossil bearing; plant debris and mica flakes; rare carbonate concretions; intact or fragmented thin-shelled bivalves; thin normally and inversely graded sand beds; pyrite; lack of abundant colloidal organic matter	**River-influenced lower offshore (prodelta)**
		FA2.1b	27-16; 27-17; 27-19; 27-20	28-8; 28-21; 28-23; 28-24; 28-31	29-14; 29-16; 29-19; 29-21; 29-26; 29-28	Clayey silt to very fine sand	Good	Reverse	Soft-sediment contorted beddings; centimeter-scale silt and very fine sand beds	Abundant; dispersed	Pervasive	Macroscopic plant-lignite debris and mica grains; abundant benthic foraminifers; rare gastropod and bivalve shell fragments; pyrite	**Storm-influenced lower offshore**
	FA2.2—Upper offshore deposits	FA2.2a	27-9	28-11		Silt to fine sand	Variable	Reverse	Parallel and climbing ripple laminations; centimeter-scale reverse and normal grading with low-angle lamination above swaley scoured surfaces	Trace	Weak	Abundant plant debris; scattered pebbles and granules; millimeter- to centimeter-scale fining-up silt and very fine sand beds	**River-influenced upper offshore (prodelta)**
		FA2.2b	27-15	28-22; 28-25; 28-29	29-20; 29-22; 29-23; 29-27	Silty clay to medium sand	Variable	Reverse	Low-angle planar laminations; hummocky cross-stratification; ripple cross-laminations	Trace	Strong; underlines internal erosion surfaces	Abundant macroscopic plant debris and mica grains; granules; gastropod and bivalve shell fragments; shell beds; benthic foraminifers; millimeter- to centimeter-scale fining-up sand beds and shell layers	**Storm-influenced upper offshore**

(*continued*)

TABLE 1. SUMMARY OF THE MAIN LITHOFACIES AND LITHOFACIES ASSOCIATIONS RECOGNIZED IN HOLES M0027, M0028, AND M0029 ON THE NEW JERSEY SHELF, WITH THEIR DEPOSITIONAL ENVIRONMENT INTERPRETATIONS (*continued*)

Lithofacies association			Lithofacies			Lithology			Sedimentary structures	Glauconite content	Bioturbation	Observations	Comments
			M0027	M0028	M0029	Grain size	Sorting	Grading					
FA3—Lower shoreface deposits		FA3.1	27-10	28-13; 28-14; 28-27	29-24; 29-25	Silt to medium sand	Good	Reverse	Current ripple lamination; low-angle oblique laminations; hummocky cross-stratification capped by mud lamina; symmetrical-aggradational ripple laminations at top of beds	Trace	Moderate	Rich in coarse sand, mica, and macroscopic plant debris; granules; shell hash layers;	**Abundant plant debris and mica**
		FA3.2		28-17; 28-19		Muddy silt to medium sand	Poor	Reverse	Hint of laminations delineated by shell lags	Abundant	Weak	Shell hash layers; scattered plant debris; benthic foraminifers;	**Abundant glauconite**
FA4—Upper shoreface deposits		FA4.1	27-11; 27-12	28-15; 28-28	29-29; 29-30; 29-31	Medium to coarse sand	Good	Reverse	Massive; high-angle trough cross-bedding; low-angle laminations; remnant of deeply scoured or cemented channelized erosion surfaces	Trace	Weak	Subangular granules; mica, wood, plant debris; dispersed shell fragments;	**Abundant plant debris and micas**
		FA4.2	27-13	28-18		Medium to very coarse sand	Poor	Reverse	Massive; sparse high-angle cross-bedding	Abundant; concentration increase upward	Weak	Granules; dispersed shell fragments; scoured surfaces underlined by coarse quartz sand lamina; local carbonate-cemented horizons	**Abundant glauconite**
FA5—Gullies and clinoform-edge fans				28-20; 28-26		Coarse sand intercalated with clay beds or lamina	Poor	Reverse	Massive; numerous internal erosion surfaces	Abundant; concentration increase upward; glauconite-filled burrows	Pervasive	Mix of mud, coarse sand, and gravel; low in mica and organic matter; deficient in silt to medium sand; shell molds; angular to rounded pebbles and granules; rip-up clasts	**Coarse, rapid sedimentation and incisions**
FA6—Transgressive lag deposits			27-14; 27-18	28-16; 28-30		Very coarse sand to clayey silts	Poor	Normal	Massive; sharp based	Abundant	Pervasive	Large pieces of wood and plant debris; subangular quartz and glauconite granules; large thick-walled shells; mica; benthic foraminifers; shell layers in clayey silts	**Marine ravinement**

Note: Lithofacies identifiers (e.g., 27-14) refer to lithofacies 14 in Hole M0027. Lithofacies are shown in Figure 3 and with more details in the Supplemental Files (Figs. S1–S3) (see text footnote 1).

The basal graded beds with angular quartz and rounded glauconite in inclined beds and the well-stratified succession with nannofossils in clay lamina suggest a sediment supply via sediment gravity flows (turbidity currents and debris flows) in a deep water environment (well below wave base). The apparent cross-bedding may indicate a channelized context where turbidity currents built dune-scale migrating bedforms on the toe-of-clinoform slope. Burrows and clay laminae show that the dune-scale bedforms migrated episodically, rather than from sustained flows. The sedimentary structures in the quartz-rich glauconite sands point to some winnowing of sediment at the seafloor, which may have favored the authigenesis of glauconite grains, their relative concentration, and then possibly their cementation with carbonate along irregular erosion surfaces. Sediment was likely sourced from a clinoform rollover location that may have been exposed, as the subangular nature of the quartz sand grains point to a very early burying of freshly eroded material. This basal part of FA1.1 is interpreted as a basal channel lag, recording bypass along erosion surfaces (Stevenson et al., 2015).

The upper part of FA1.1 is well organized in meter-scale graded successions, but it is still poorly sorted, with a mix of quartz, glauconite, and shell fragments with traces of dissolution in a muddy matrix. These are probable indications of downslope gravity sediment transport. The fining-upward trend together with the suite of sedimentary structures showing a progressive decrease in the energy of transport (horizontal parallel lamination, cross-bedding, and low-energy planar lamination) point to a probable channelized transport of a stack of debrites and turbidites at the toe of a clinoform slope apron. The lack of mica and plant debris is noticeable and might indicate a progressive overall retreat of the regional river outlets. The gradational thinning and fining of beds uphole indicate a possible sediment supply response to transgression in an overall marine onlap. Those facies likely were emplaced below the maximum storm wave base (i.e., 80–120 m water depth) as suggested by the lack of traces of hydraulic reworking by waves.

Slope apron deposits—FA1.2. Lithofacies association FA1.2 comprises a wide range of facies that are usually arranged as glauconite-rich decameter-

thick fining-upward successions. A distinction is made between coarse-grained deposits (FA1.2a) and the overlying silty-clay deposits (FA1.2b). **FA1.2a** is composed of stacked, meter- to 10-m-thick coarsening- and/or fining-upward successions. The coarsening-upward succession (lithofacies 27-2, 28-4, 28-5, 29-5, 29-8, 29-17) is made up of homogeneous, poorly sorted, coarse-grained quartz and glauconitic (5%–10% to 30%) sand with dispersed quartz granules, concentrations of pebbles (up to 15%), and common weak normal grading; granule and pebble grains tend to be less rounded than sand-grade grains. The fining-upward successions (27-3, 28-5, 29-3, 29-5, 29-17) are coarse- to medium-grained quartz and glauconitic (up to 25%–60%; 27-3) sand lying on a coarse basal lag with granules along an erosive or bioturbated surface. The original subhorizontal or ripple lamination with normal grading are in places largely obscured by bioturbation (e.g., *Planolites*, *Teichichnus*, *Diplocraterion*, and *Zoophycos*; 27-3) and dish, contorted, and convolute lamination. These coarsening-upward–fining-upward successions are locally interbedded with mud-supported granule and pebble sands with centimeter-thick clay beds (e.g., 29-3). Glauconite grains are a mix of pale-green (immature) granules and smaller black grains (mature). **FA1.2b** is fining-upward brown silt to silty clay with glauconitic, fine- to medium-grained sand beds, floating coarse and very coarse quartz and glauconite sand grains (29-10), foraminifers and thin-walled shells, traces of mica, and plant debris. Granules and aggregates of pale-green (immature) and subangular glauconite are observed with fine-sand grains of dark green and subrounded glauconite (mature). The sediment is moderately bioturbated with identifiable *Chondrites* and *Planolites* (Fig. 4C) and at one place a 30-cm-long *Thalassinoides* burrow (27-1). Glauconite is commonly concentrated in burrows (vertical burrows and *Teichichnus*) along erosion surfaces together with rare shell fragments, benthic foraminifers, and disseminated pyrite but including quartz granules (29-11, 29-12) or not (29-7). The sand beds form weakly normally or reversely graded layers with rare ripple-scale cross-lamination (29-4, 29-6). Thick-walled shells occur but show signs of severe dissolution (29-12).

FA1.2a facies are dominated by moderately to poorly sorted, coarse sand-prone sediment with dispersed granules and pebbles and local concentrations of gravel. Weak normal grading supports the partial transformation of debris flows into high-density turbidity currents, but the general poor sorting can be attributed to mixing through bioturbation and/or cohesive debris flow deposition, as shown by the presence of muddy sand with floating granules and pebbles. Centimeter-thick clay and sand interbeds might represent waning-stage deposits. These poorly sorted coarse sediments are interpreted as high-concentration flows of coarse material eroded from updip positions settled at the toe of a clinoform slope apron. These facies may correspond to simple coalesced toe-of-slope fans. The presence of micas and plant debris in the finer **FA1.2b** is indicative of a distant but quasi-permanent river sediment input on the shelf. The abundance, in places exclusive (29-7), of glauconite grains—either (1) dark green, well-rounded and subangular, and broken, or (2) pale green, in situ aggregates—as well as thick shells with traces of dissolution (29-12), points to temporary local deep marine starved conditions. The common concentration of the glauconite grains, together with foraminifers or quartz sand grains, in burrows along erosion surfaces points to occasional current-swept floor conditions, which probably in turn favors the generation of the glauconite. The glauconite grains can be produced both in situ or reworked from the clinoform slope (e.g., Hesselbo and Huggett, 2001). The common occurrence of fining-upward, centimeter- to decimeter-thick sand beds (29-10, 29-12), or thick mud (29-7) with floating coarse (29-10) to granule-size (29-12) quartz and glauconite grains clearly indicates either a component of downslope transport of clastic sediment in dilute turbidity currents or a stack of poorly mature, cohesive(?) debris flows provided by the slope of a clinoform. Overall the decameter-thick vertical stack of FA1.2a and FA1.2b corresponds to the development of fans on the bottomsets of clinoforms that develop below the maximum storm wave base (i.e., 80–120 m water depth) as suggested by the lack of traces of hydraulic reworking by waves.

Storm- and River-Influenced Offshore Marine Deposits—FA2

Offshore marine deposits consisting of marine silts and silty clays are widely distributed in the three holes. They encompass a large number of facies deposited below storm wave base (lower offshore, FA2.1) and between fair-weather and storm wave base (upper offshore, FA2.2). In the literature, this "upper offshore" domain is often termed the "offshore-shoreface transition" (as used by Mountain et al. [2010b]). In cores, lower (FA2.1) and upper (FA2.2) offshore deposits are either river- (FA2.1a, 2.2a) or storm- (FA2.1b, 2.2b) influenced.

River flood–influenced deposits. The river-influenced deposits consist of coarsening- and thickening-upward meter- to 10-m-thick successions of silty clay to fine to medium quartz sand with abundant mica, plant debris, shell fragments (lithofacies 28-3, 28-12), sponge spicules, and diatoms. The silty clays (**FA2.1a**) are nannofossil bearing. They can be tan colored (29-2) showing micro-laminated clay-rich layers (28-12). Sandier beds are parallel or ripple laminated, and normally (28-3, 28-10, 28-12) to inversely graded (28-3, 28-10) with gradational boundaries (28-3). Bioturbation is absent in clay-rich layers but obscures laminations in sands. Identified frequent burrows include *Chondrites* and *Planolites* but are predominantly simple meniscate backfilled forms, e.g., *Teichichnus* (29-2) or *Taenidium* (Fig. 4A), filled by glauconite (28-3) or replaced by pyrite that may mimic fecal pellets (?*Ophiomorpha*). Also present are common precompactional carbonate concretions (29-2, 28-3, 27-7, 28-3). The silt to fine sands (**FA2.2a**) show abundant plant debris, scattered pebbles and granules (28-11), parallel and climbing ripple lamination, and centimeter-scale reverse and normal grading, with low-angle lamination above a swaley scoured surface.

FA2.1a lacks abundant colloidal organic matter, but the abundance of plant debris and mica indicates a fluvial source for the sediment. The well-laminated silty clays suggest that the depositional environment was probably very quiet and periodically subject to dysoxic bottom waters, as shown by the presence

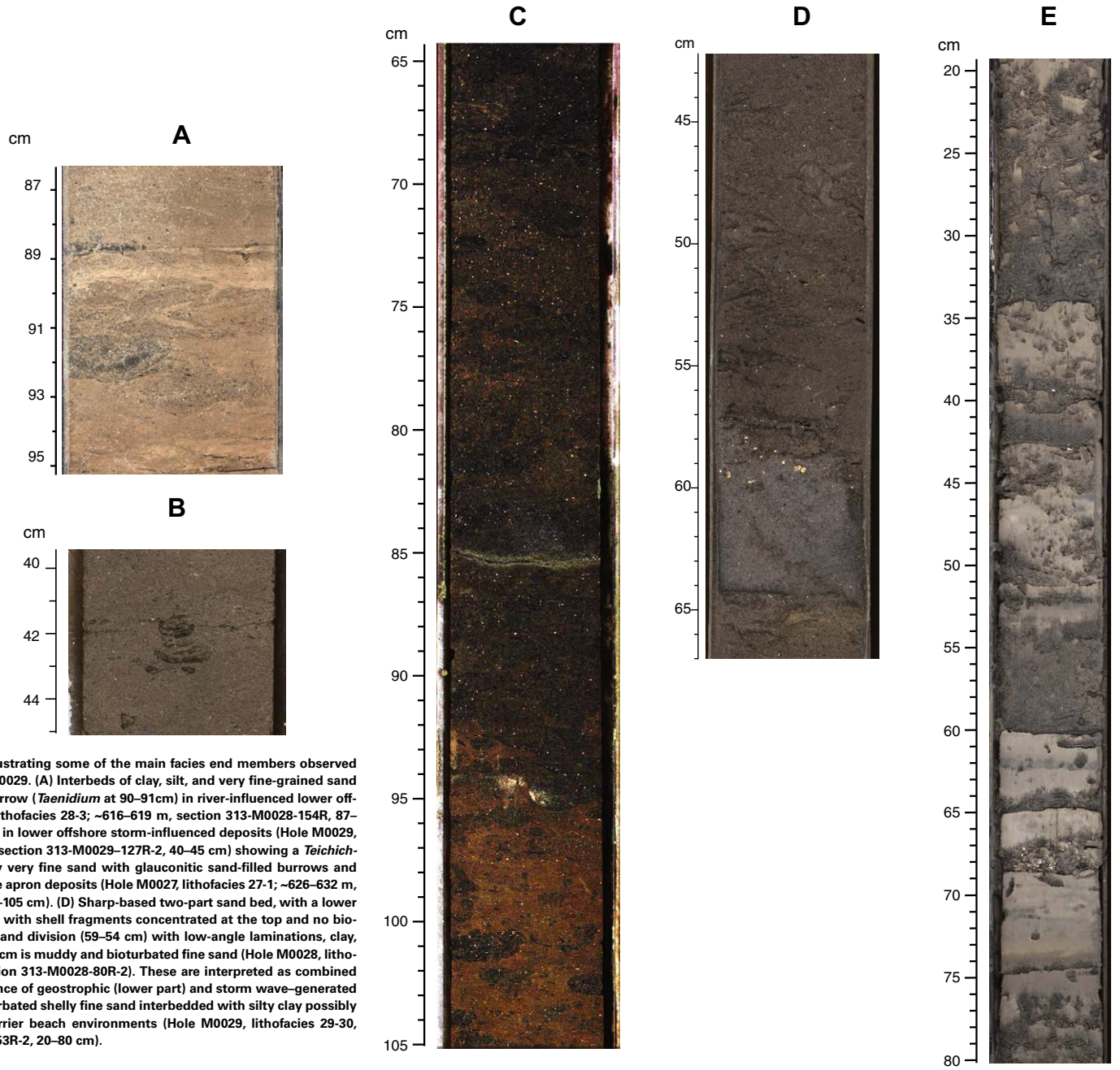

Figure 4. Core photographs illustrating some of the main facies end members observed in Holes M0027, M0028, and M0029. (A) Interbeds of clay, silt, and very fine-grained sand with a meniscate backfilled burrow (*Taenidium* at 90–91cm) in river-influenced lower offshore deposits (Hole M0028, lithofacies 28-3; ~616–619 m, section 313-M0028-154R, 87–95 cm). (B) Silty very fine sand in lower offshore storm-influenced deposits (Hole M0029, lithofacies 29-16; ~505–507 m, section 313-M0029–127R-2, 40–45 cm) showing a *Teichichnus* burrow at 42 cm. (C) Silty very fine sand with glauconitic sand-filled burrows and *Chondrites* in the starved slope apron deposits (Hole M0027, lithofacies 27-1; ~626–632 m, section 313-M0027–223R-1, 65–105 cm). (D) Sharp-based two-part sand bed, with a lower clean sand division (64–59 cm) with shell fragments concentrated at the top and no bioturbation, and an upper silty sand division (59–54 cm) with low-angle laminations, clay, and no bioturbation. Above 54 cm is muddy and bioturbated fine sand (Hole M0028, lithofacies 28-13, ~417–420 m, section 313-M0028-80R-2). These are interpreted as combined flow deposits under the influence of geostrophic (lower part) and storm wave–generated (upper part) currents. (E) Bioturbated shelly fine sand interbedded with silty clay possibly deposited in lagoonal and barrier beach environments (Hole M0029, lithofacies 29-30, ~288–292, section 313-M0029-53R-2, 20–80 cm).

of concretions that excluded burrowing fauna. At times of better oxygenation, the infauna was dominated by horizontally mining deposit-feeding organisms. The gradational upper and lower boundaries and local basal reverse grading of the very fine, parallel- and ripple-laminated sand beds, as well as the millimeter-scale clay-silt laminations in the clay, point to a river flood origin of deposition with a possible seasonality. The depositional environment is interpreted as river-dominated lower offshore (prodelta) settings. **FA2.2a** shows indications of hydraulic sediment transport on the seafloor (parallel, climbing ripple lamination) and also the possible distal influence of storms (low-angle lamination on swaley scoured surfaces) indicative of a progressive shallowing from the lower to the upper offshore environments.

Low-energy, storm-influenced deposits. The storm-influenced deposits consist of coarsening-upward, meter- to 10-m-thick successions of silty clay to quartz and glauconitic sands with gastropods (e.g., *Turritella*), thin-walled bivalve shell fragments, and benthic foraminifers. The clayey silt to silty clay (e.g., 27-16, 28-8, 28-21, 28-23) (**FA2.1b**) contains abundant dispersed glauconite sand grains and macroscopic plant debris and mica grains, landward of clinoform rollover points (e.g., 27-16, 27-17). In the upper part of the three holes is a dark brown massive clay with abundant benthic foraminifers, rare shell fragments, faint lamination defined by weak concentrations of plant debris, bioturbation (*Planolites*), and scattered calcilutite beds (27-17), and a pale and gray-yellow-brown color-banded clay with *Chondrites*, pyritic and silty laminae, and common soft-sediment contorted bedding at different scales (28-31, 29-26). Sporadic millimeter- to centimeter-scale silts and very fine sand beds with faint laminae and a fining-upward trend are locally present within the silty clay (e.g., 27-19, 29-16). Bioturbation is usually pervasive (29-14, 29-16, 29-21), and burrow infills locally contain coarse glauconite and quartz sand or granules (e.g., 29-16). The thoroughly bioturbated silty clays are interbedded with coarsening- (28-25) or fining-upward (28-22, 29-22, 29-27) successions of centimeter-scale, silty to very fine sand beds (**FA2.2b**). Bioturbation is pervasive in silty clay beds and also underlines erosion surfaces (*Chondrites*, *Planolites*, *Cylindrichnus*, *Teichichnus* burrows; Fig. 4B) (27-15, 29-23) or crosscuts the lamination (28-22). Sand beds are normally graded (29-22, 29-23) with low-angle shell layers (28-25, 29-20), hummocky cross-stratification (27-15, 28-22), and ripple and low-angle cross-laminations (28-29). FA2.2b typically overlies FA2.1b; together they form meter- to decimeter-thick coarsening-upward stacks of facies.

The silty clay material of facies **FA2.1b** shows indications of deep lower offshore marine conditions with an abundant autochthonous fauna and active bioturbation, and episodic starvation (in situ glauconite), but no trace of hydraulic reworking by wave action. In places, the banded character of the clays with *Chondrites* and pyrite and the presence of calcilutite beds confirm periodic sediment-starved bottom conditions. Color banding in clays underlines discrete depositional events that are interpreted as low-density turbidity currents possibly triggered by storm events. Occasional downslope sediment transport is suggested by the presence of sporadic fining-upward centimeter-thick sand beds. Deformation of cohesive sediment indicates some instability of the seafloor, and a clastic sill near the base of the clays may relate to overpressure in underlying sands. The mixing of mud with sand-size glauconite grains might imply some reworking from upslope of poorly mature, cohesive(?) debris flow deposits with burrowed erosive surfaces indicative of exposure of the seafloor between two successive sedimentation events. The heterolithic nature of **FA2.2b** points to upper offshore conditions with alternating quiet environment and reworking or downslope transport processes. The occurrence of well-sorted, fining-upward sand beds and shell layers with low-angle and ripple laminations are indicative of hydraulic reworking of the seafloor by the distal influence of storm waves (i.e., storm-graded layers) in slightly shallower waters than FA2.1b in upper offshore environment. The meter-scale coarsening-upward trends point to probably recurrent periods of shoaling from the lower to the upper offshore environments. Paleoenvironmental reconstructions suggest that FA2.2b facies were deposited below maximum fair-weather wave base (i.e., 20–30 m water depth) and above maximum storm wave base (i.e., 80–120 m water depth).

Lower Shoreface Deposits—FA3

The lower shoreface facies form regular coarsening-upward progradational successions at the toe of the shoreface. They are of two types, depending on their content in plant debris and mica (FA3.1) and in glauconite (FA3.2).

FA3.1 is rich in coarse sands, micas, and macroscopic plant debris. It is located in the middle part of Hole M0027 (332–337 m, 375–415 m) and the lower part of Hole M0028 (400–440 m). It shows coarsening- and thickening-upward successions of moderately bioturbated silts to well-sorted medium quartz sand with granules (lithofacies 27-10, 28-13, 28-14, 28-27). There are many distinctive two-part sand beds in the lower part showing a slight grain-size change at the lamina scale (28-13). These beds have sharp bases overlain by clean quartz sand (no silt or mica) and silty sand with subparallel low-angle lamination (Fig. 4D), current ripple laminations, and symmetrical-aggradational ripples at the top. Shells and plant debris are concentrated near the tops of beds (Fig. 4D), which are typically bioturbated (28-13). Shell hash layers increase upward along low-angle slightly erosive soles (28-14) or thick-thin beds (27-10). In the latter, thick beds with low-angle oblique lamination or hummocky cross-stratification, capped by mud laminae, alternate with intensely bioturbated horizons. Less-bioturbated places show some distinctive burrows such as *Cylindrichnus*, *Thalassinoides*, and *Teichichnus*. **FA3.2** is rich in glauconite grains. It is found in the upper part of Holes M0028 and M0029. It comprises coarsening- and thickening-upward, meter- to decimeter-scale successions from muddy, glauconitic silt to medium quartz sand (28-17, 28-19). Hints of laminations are delineated by shell lags (28-17–28-19).

The abundance of mica and plant debris in **FA3.1** suggests that the supply had a strong fluvial influence. The two-part sand beds are interpreted as combined-flow storm deposits in a high-sediment-supply environment. The lower clean and slightly coarser quartz sand is interpreted as having been deposited

from geostrophic (unidirectional) currents that transported sediment entrained from the coeval shoreface to deeper water, as is commonly observed in subaqueous deltas (Mitchell et al., 2012; Patruno et al., 2015b). The upper sediment was locally agitated, and deposits from (orbital) currents set up by storm waves formed low-amplitude hummocks, current ripples, and late-stage symmetrical (wave) ripples before organisms could start to mix the sediment again. The succession overlies upper offshore FA2.1a and FA2.2a stacks and is interpreted as having been deposited at the toe of the shoreface in a river-influenced setting at water depth ranging from 10 to 20–30 m. The presence of glauconite grains and the overall absence of plant debris in **FA3.2** suggest reduced river sediment supply as compared with FA3.1.

Upper Shoreface Sand Deposits—FA4

Upper shoreface facies comprises quartz-rich sand successions (FA4.1) overlying facies FA3.1, and glauconite-rich sand (FA4.2) overlying FA3.2.

FA4.1 is thick-bedded, coarsening-upward, medium- to coarse-grained quartz sands with subangular granules. The sediment is poorly sorted. It includes mica, wood and plant fragments (lithofacies 27-11, 27-12, 29-29), subangular granules (28-15, 28-28), black non-organic grains, and dispersed shell debris. The sand usually appears homogeneous and loose with remnants of deeply scoured (28-15, 29-29) or cemented channelized erosion surfaces (27-12). Sedimentary structures are faint and, when preserved, show high-angle trough cross-bedding and low-angle laminations (27-11, 27-12). Bioturbation is represented by distinctive *Cylindrichnus* backfilled burrows (27-11, 27-12). In the upper part of Hole M0029 (29-29, 29-30, 29-31), the stack of coarsening-upward trends is capped by interbedded, centimeter-scale, sharp-based, bioturbated blue-gray silty clay and well-sorted, medium to fine sand showing in places ripple cross-lamination (Fig. 4E). **FA4.2** is thick bedded, poorly sorted, coarsening-upward, medium- to very coarse-grained glauconite-rich (up to 20%) quartz sand with granules (27-13) and dispersed shell debris (28-18). Glauconite content tends to increase upward from 1%–3% to as much as 20%. Sedimentary structures are usually poorly preserved and the sand appears homogeneous and loose (28-18), although sparse high-angle cross-bedding and scoured surfaces are locally underlined by coarse quartz sand laminae (27-13). Sparse vertical burrows and local carbonate-cemented horizons are recorded along internal discontinuities.

The coarse-grained, thick-bedded coarse sand with subangular granules and high-energy sedimentary structures (high- and low-angle cross-bedding, scouring) of both facies associations are typical of prograding wave-influenced shoreface sediment bodies. The abundance of mica flakes, angular granules, and wood fragments (**FA4.1**) points to the proximity of a river feeder at the top of the shoreface or delta lobe sands as shown by the presence of channelized scours (e.g., 27-12) in Hole M0027. The more massive and loose character of sand of **FA4.2** together with high glauconite content might indicate the deposition of sediment rapidly transported across (bypassing?) the shelf from outer estuarine environments to the rollover. These sands deposited below fair-weather wave base at the rollover recall the sand-prone subaqueous clinoform facies of Mitchell (2012), Mitchell et al. (2012), and Patruno et al. (2015b).

Gully and Clinoform-Edge Fan Deposits—FA5

Facies association FA5 underlines seismic unconformities m5.2 (ca. 15–15.6 Ma; Browning et al., 2013) and m5 (ca. 13.7 Ma) (Fig. 2) landward of clinoform rollover points and overlies FA4.2 facies in Hole M0028. It comprises crudely coarsening-upward, coarse glauconite sand (up to 40%) intercalated with clay beds (lithofacies 28-26) or lamina (28-20). FA5 is poorly sorted and dominantly coarse grained, with a mix of mud, sand, and gravel. Generally, sediment is low in mica and organic matter and deficient in silt to medium sand grain sizes compared to the surrounding stratigraphy. Overall, the succession becomes more glauconitic (up to 40%) and increasingly stratified uphole, with highly bioturbated mud-rich units with gravel layers or weakly graded beds. FA5 shows numerous internal erosion surfaces overlain by (1) weakly fining-upward and bioturbated gravel-rich sand and sandstone with complete benthic foraminifera (28-26), and (2) 0.1–0.2-m-thick matrix-supported, muddy glauconitic (up to 40%) poorly sorted coarse sand with up to 20% quartz completed by lithic and mud granules and pebbles, and scattered pyrite grains, lacking shells but containing molds. Granules and pebbles are well rounded to angular. Bioturbation is pervasive, with mud- and glauconite-filled burrows (28-20). Mud pebbles exhibit bioturbation identical to that of the host bed (28-20).

The poorly sorted sand with mud and gravel, with shell molds and rip-up clasts, indicates erosion and reworking in a marine setting. Rounded clay clasts that have a bioturbated fabric are interpreted as intraclasts entrained from the substrate. The weak grading of some deposits supports waning sediment gravity flows. Possible interpretations of these deposits at the clinoform rollover include gully fills for the fining-upward successions and/or outbuilding of small deltas with steep fronts for the coarsening-upward trends that formed during periods of lowering relative sea level. The lack of plant debris and mica and the low proportion of very fine to medium sand compared to the surrounding stratigraphy suggest that these components may have been transported downdip, with the coarser material and muds from eroded surrounding substrate preferentially retained. The extent of the drainage basin that fed the deltas and/or gullies is not clear. However, the source for the coarse extrabasinal material need not to be tied directly to the hinterland and may have been from older deposits.

Transgressive Lag Deposits—FA6

Facies association FA6 lies on erosion surfaces at the topset of clinoforms and underlines seismic surfaces m5 (ca. 13.7–14.8 Ma; Browning et al., 2013), m5.2 (ca. 15–15.6 Ma), m5.3 (ca. 16.3–17.3 Ma), m5.32 (ca. 16.7–17.4 Ma), m5.4

(ca. 17–17.7 Ma), and m5.45 (ca. 18 Ma) in Hole M0027, and m4.1 (ca. 12.9 Ma) in M0028 (Figs. 2 and 3). FA6 is composed of massive, sharp-based, decimeter- to meter-scale, usually fining-upward successions from (1) clean, coarse to very coarse glauconitic and quartz sand with subangular quartz and glauconite granules to (2) bioturbated fine sand, containing moderately sorted medium sand, with large pieces of wood and plant debris, large thick-walled shells, mica (2%), benthic foraminifers, and clay-filled burrows, and (3) clayey silts with dispersed organic matter, isolated sand grains and granules, common shell layers (bivalves and gastropods), foraminifers, diatoms, and sand-filled burrows (lithofacies 27-18). Bored cemented sand nodules with glauconitized rims and *Thalassinoides* burrows going down to 25 cm filled by coarse sand and granules are observed, in places, along erosion surfaces (27-14, 28-16, 28-30).

The coarse-grained sediment with large, thick-walled shell and wood debris originates from a very proximal and high-energy shoreface environment close to a river outlet. The poor sorting with a mixing of granules with fines, arranged in both fining- and coarsening- upward trends, point to a transport mechanism by a mix of sediment traction and gravity flows along the erosional surfaces. The lack of clayey material suggests some reworking by wave energy in a depositional environment close to the toe of the shoreface. Coarse to fine sand with bored nodules and glauconite grains are indicative of condensed deposition and subsequent erosion and exhumation. These sediments underlining erosion surfaces are interpreted as relics of ravinement deposits associated with sea-level rise and transgression.

Seismic Stratigraphic Architecture

The interpretation of the New Jersey shelf seismic data showed that the early and middle Miocene sediment pile can be divided into 18 seismic units or clinothems bounded by unconformities of regional lateral extent designated by the name of their underlying unconformity (m6–m4.1; Monteverde et al., 2008) (Figs. 2 and 5A). In their regional study, Monteverde et al. (2008) distinguished two packages of reflectors on the New Jersey shelf, interpreted as lowstand and highstand systems tracts. The detailed observation of the 2-D seismic line 529 of cruise Oc270 led us to individualize four sets of reflection packages in the seismic units (Figs. 5, 6, 7, and 8) based on their shape and the internal reflector terminations and configurations. From base to top, the sets are the following:

- Set 1—A lens-shaped unit bounded at the base and top by high-amplitude reflectors onlapping the toe of the clinoform front. The set is transparent to reflection free.
- Set 2—A wedge- to lens-shaped unit largely sitting on the shelf with high-amplitude reflectors at the base and top, and more locally (distally) sitting on the bottomset or foreset of clinoforms. Internal reflectors show onlap and downlap basal terminations and toplap terminations at the top. Reflectors show high amplitude, good continuity, and low frequency on the shelf. The configuration is subparallel on the shelf, and low-angle oblique tangential seaward, in the clinothems.
- Set 3—A slope-front fill unit with a bank to lens shape. Reflectors show moderate-angle downlap terminations and local onlaps, or are conformable at base, and show erosional or apparent truncations at top. Internal reflectors show a mix of high- and low-amplitude reflections, low to moderate continuity, and low frequency. The configuration is complex oblique to chaotic.
- Set 4—A slope-front fill unit with a lens shape. Reflectors exhibit onlap-downlap terminations, locally conformable at the base and with apparent truncation at the top. Internal reflectors are of moderate to high amplitude and largely discontinuous, with a moderate frequency. The configuration is tangential oblique to complex oblique sigmoidal.

Sedimentary Facies Architecture

Preliminary ties were established between the cores, the holes (through downhole logs), and the Oc270–529 seismic line (Fig. 2) during Expedition 313 (Mountain et al., 2010b) and refined by Miller et al. (2013b). A reappraisal of these ties according to sedimentological observations made in this study provide the opportunity to correlate corehole facies interpretations from one hole to another (Fig. 3) and along the regional 2-D dip section following geometries observed on the seismic line (Fig. 7).

Clinothem Units

The individual seismic units appear basically composed of a deepening (transgressive) and a shallowing (regressive) suite of facies made up of coarse-grained debrites overlain by a progradational stack of lower to upper offshore, and shoreface sediments (Fig. 7; see a sketch of a typical clinothem units in Fig. 8). In detail, however, each set of seismic reflectors in the seismic unit shows a specific suite of facies or systems tract in cores (Figs. 7 and 8). Seismic set 1 comprises amalgamated debrite deposits (lithofacies association FA1.1) at the toe of the slope and transgressive lag deposits (FA6) on the topset of clinoforms. Seismic set 2 is well represented on the shelf but rarely recognized at the toe of the slope. It shows lower offshore sediments (FA2.1) giving rise upsection to upper offshore deposits (FA2.2). Seismic set 3 forms the bulk of the clinothems. It shows a large suite of facies from slope apron fans (FA1.2), to lower (FA2.1) and upper offshore deposits (FA2.2), giving rise to lower shoreface sediments (FA3). Gully-fill deposits (FA5) are observed twice capping set 3 deposits landward of the rollover. Seismic set 4 exhibits a large range of facies and the shallowest depositional environments. It shapes the rollover and drapes the slope. It comprises lower offshore to upper shoreface deposits (FA2.1 to FA4).

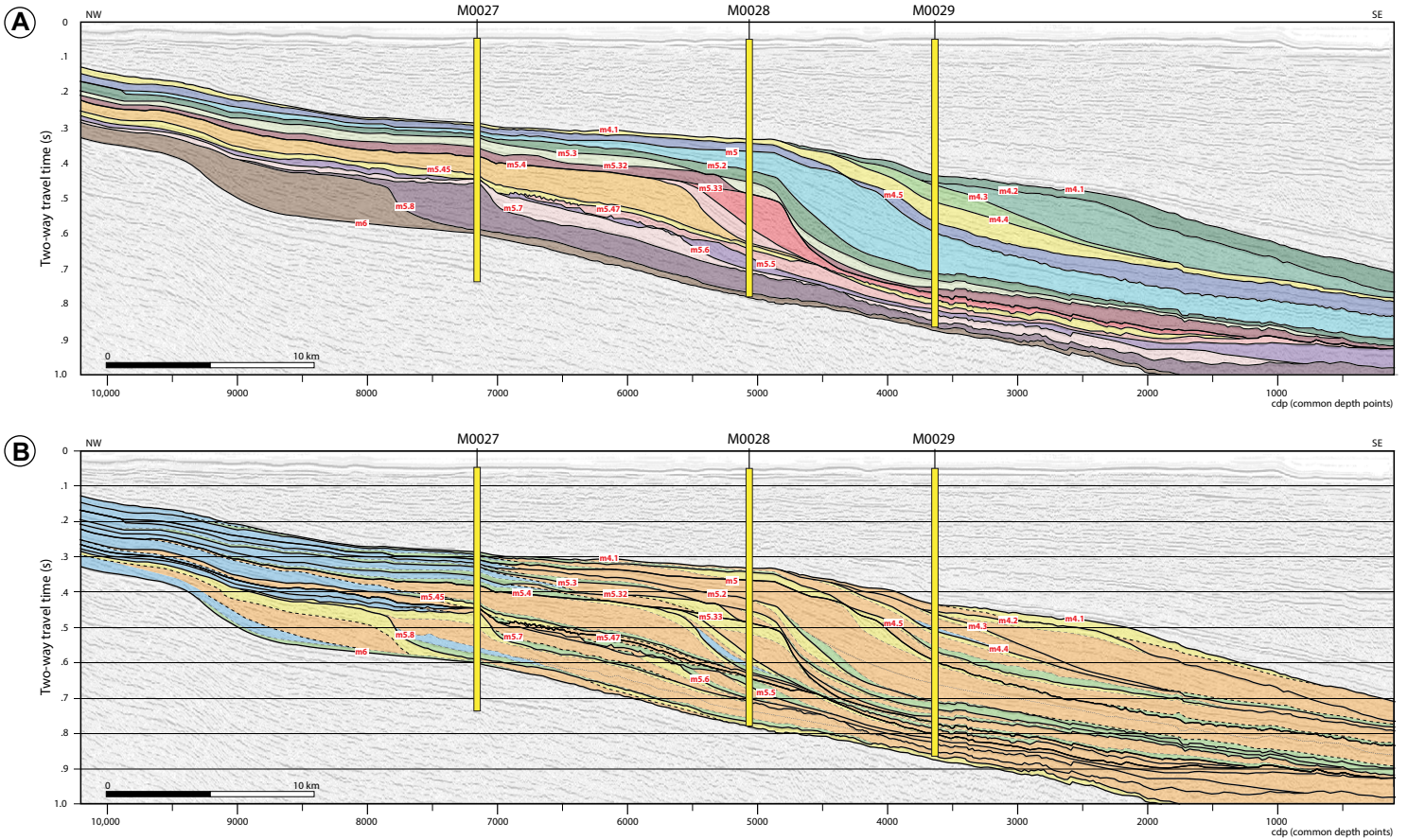

Figure 5. Interpretation of R/V *Oceanus* cruise Oc270 seismic line 529 showing the main seismic units as successively revised by numerous authors (e.g., see Monteverde et al., 2008; Mountain et al., 2010b; Miller et al., 2013a, 2013b; Browning et al., 2013) including this paper (colors delineate the different seismic units) (A), and the distribution of the sets or seismic reflectors (i.e., systems tracts) in the seismic units (see Fig. 7 for colors of sets) (B).

Key Bounding Surfaces

The seismic sequence boundaries (e.g., m5.8–4.1; Fig. 7) are the most prominent surfaces that bound the clinothem units in the coreholes (see Miller et al. [2013b] for a detailed description). They are sharp, erosional surfaces separating shallow marine facies below from deeper marine facies above (see a sketch of a typical clinothem unit in Fig. 8 and details in Fig. 3 and the Supplemental Files [Figs. S1, S2, and S3; footnote 1]). On the shelf, these surfaces are underlain by poorly sorted, immature sand material (transgressive ravinement deposits, lithofacies association FA6). At the toe of the slope, they are overlain by amalgamated sediment gravity flows (FA1.1), which progressively wedge out further seaward where the surfaces become conformable. The seismic set boundaries within the seismic units can also be delineated in cores. The surfaces at the boundary between seismic sets 1 and 2 correspond to a change from fining-upward to coarsening-upward trends at the deepest paleoenvironments, the finest-grain-size horizon, and gamma-log peaks. The surfaces at the boundary between seismic sets 2 and 3 and sets 3 and 4 are less straightforward in cores than on seismic lines. A seaward shift of the facies (i.e., systems) tracts and, in places, a sharp increase in grain size explains the high amplitude of the reflectors and characterizes the changes in the angle of the reflectors between the seismic sets on seismic lines.

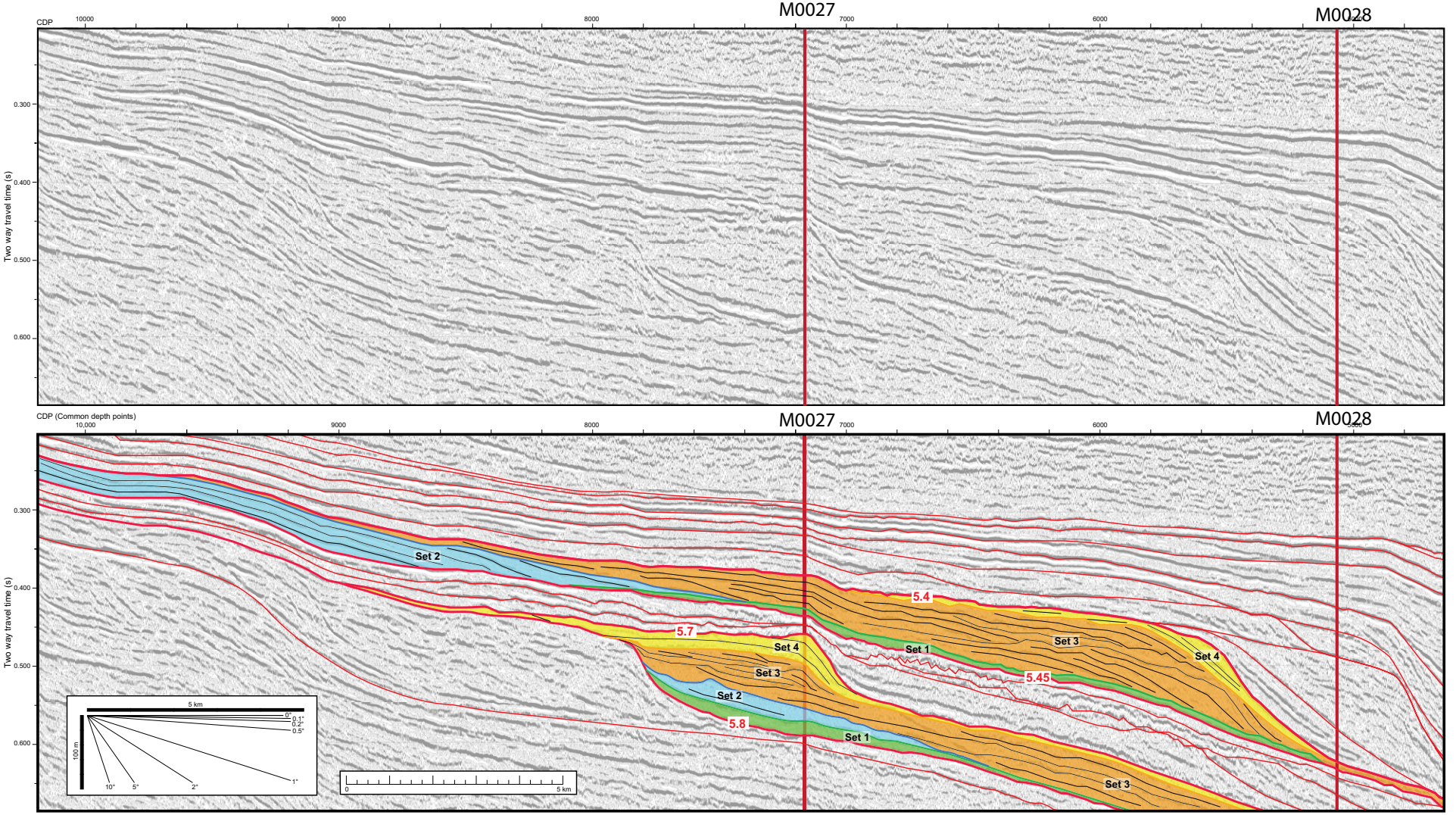

Figure 6. Uninterpreted and interpreted views of part of R/V *Oceanus* cruise Oc270 seismic line 529 showing the distribution of the sets of seismic reflectors in seismic units m5.8 and m5.45 (see Fig. 7 for colors of sets). Inset at the lower left corner is a dip angle guide to estimate the dip of the seismic reflectors.

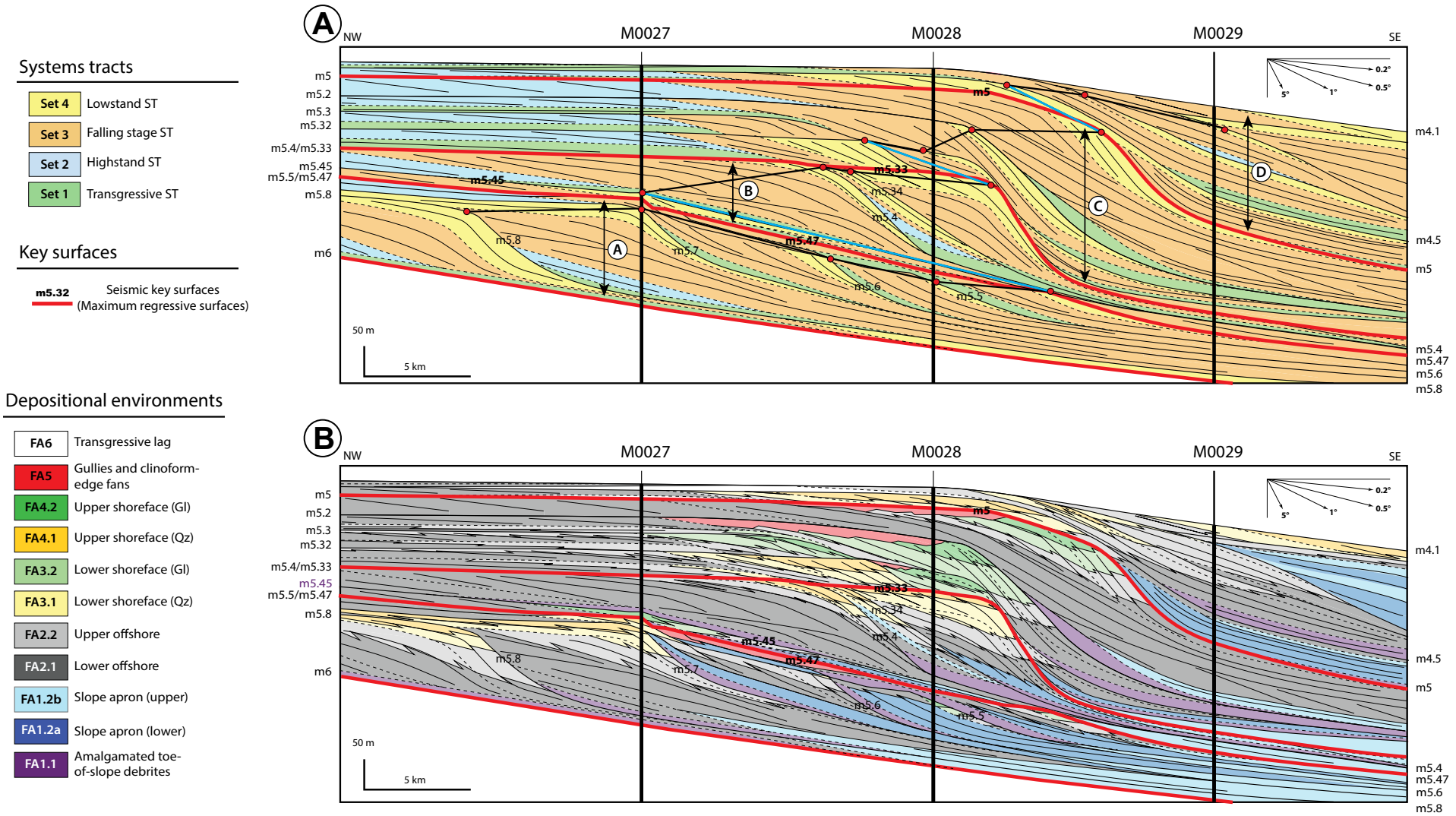

Figure 7. R/V *Oceanus* cruise Oc270 seismic line 529 with superposed Holes M0027, M0028, and M0029 (see Fig. 1 for location) and seismic unit boundaries interpreted by Monteverde et al. (2008), Mountain et al. (2010b), and Miller et al. (2013a, 2013b). The figure shows (A) the lateral distribution of the systems tracts (STs), seismic units (sets), and stacks of units (A to D). (B) Lateral distribution of the depositional environments interpreted from the drill core analysis and correlation from hole to hole, within the unconformity-bounded seismic units. Unconformity names (m5 to m6) are as proposed by Monteverde et al. (2008). See text for details. Insets at the upper right corners are dip angle guides to estimate the dip of the seismic reflectors. Gl—glauconite; Qz—quartz.

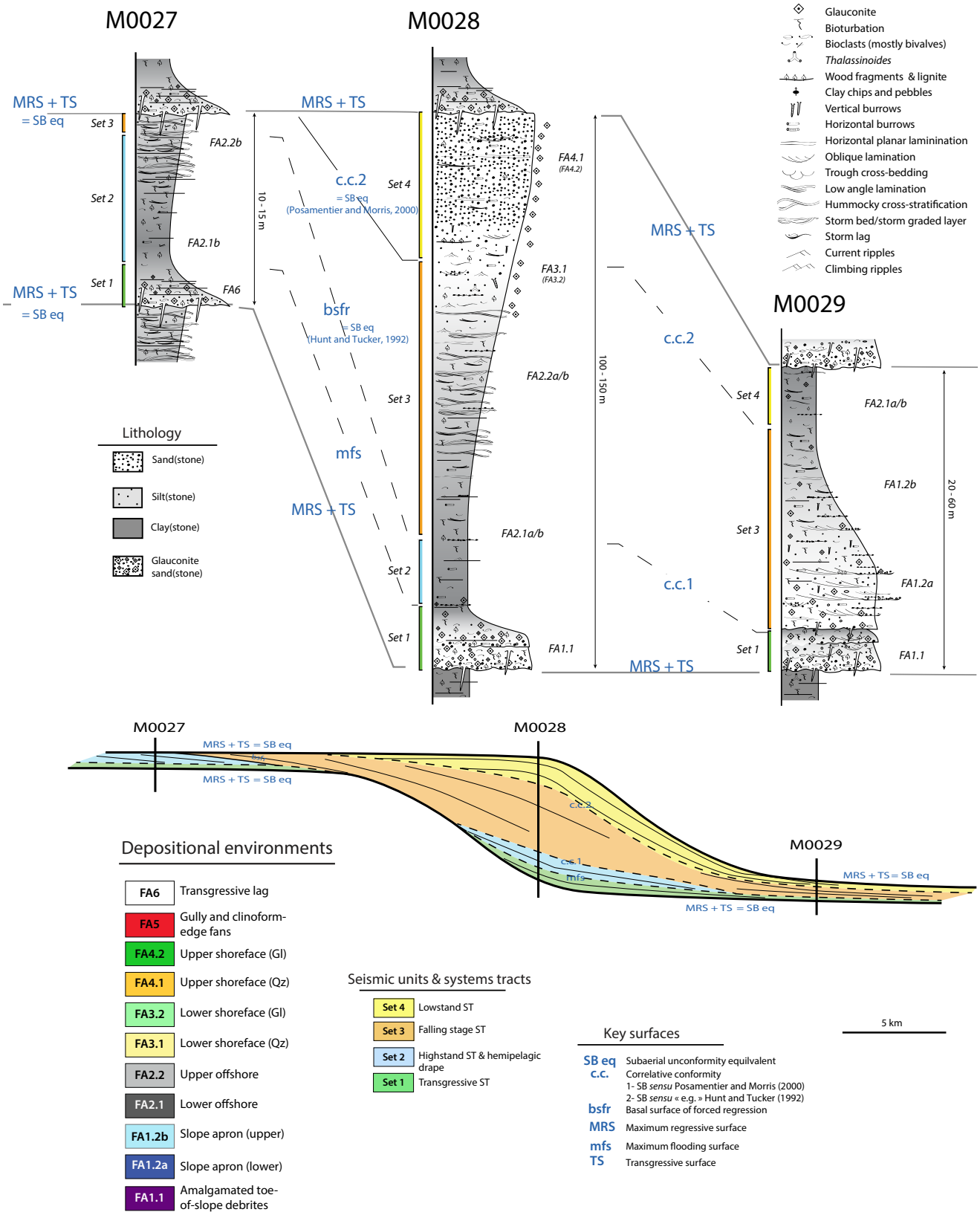

Figure 8. Simplified sketch showing the sedimentary architecture of a typical lower to mid-Miocene clinothem seismic unit as observed in the three coreholes M0027, M0028, and M0029 drilled on the New Jersey shelf. The lower Miocene units exhibit thick accretion shoreface bodies building up large river-influenced delta lobes, while the middle Miocene units are composed of thinner, sharp-based shoreface deposits in wave-dominated settings. Depositional environments are interpreted from the analysis of facies associations (FA; see text for a description). Systems tracts (ST) are interpreted from the stacking pattern of facies associations bounded by key surfaces tied to seismic units (see text for a description). Gl—glauconite; Qz—quartz.

Stacks of Clinothem Units and Clinoform Trajectory Analysis

Despite the lack of 3-D control on geometries, the 2-D seismic section displays the gross sediment architecture of the stack of New Jersey margin clinothem units (Monteverde et al., 2008). As shown on Figure 7A, and following Helland-Hansen and Hampson (2009), the trajectory of the clinoform rollovers shows repeating features that characterize different stacks of clinothem units (stacks A to D, Fig. 7A). Each stack exhibits a landward shift of the clinoforms' break in slope followed by a seaward shift, which correspond respectively to a retrogradational and a progradational stacking pattern of the clinothem units into a larger-scale transgressive-regressive (T-R) sequence. Each T-R sequence is underlain on the topset by an erosional surface at the maximum regression that corresponds to the transgressive surface of the classical stratigraphic sequences. This surface is overlain by transgressive ravinement deposits (lithofacies association FA6) on the shelf, glauconitic shoreface sands (FA3, FA4) at the rollover, and submarine fan debrites (FA1.1) of the healing phase at the toe of the clinoform slope. In places, the surface can go through the debrites facies (Hodgson et al., 2018). The early stage of the progradational part of the T-R sequence comprises offshore marine silts and clays enriched with mica and wood fragments sourced by rivers (FA2) while the late stage of the progradation shows relatively clean and sandier lower (FA3) to upper shoreface (FA4) material influenced by permanent wave action giving rise downslope to slope apron sediment gravity flows (FA1.2).

DISCUSSION

Clinoforms are a common structure of continental margins in a number of settings and a key component of sedimentary successions used to interpret the interplay between changes in relative sea level and sediment supply (Vail et al., 1977; Posamentier et al., 1988; Van Wagoner et al., 1990). A review of the literature shows that different scales of progressively large-scale clinoforms can prograde simultaneously along a transect from the shoreline to the abyssal plain, merging to form compound clinoforms, depending on changes in sediment supply, sea level, and subsidence (Helland-Hansen and Hampson, 2009; Henriksen et al., 2009; Swenson et al., 2005; Patruno et al., 2015a). Expedition 313 focused on the intermediate-scale clinoforms located on the shelf (Hodgson et al., 2018; Mountain et al., 2010a, 2010b), between (1) the (subaerial) shoreline delta and its subaqueous or prodelta counterpart, of a few meters to tens of meters high, formed by T-R processes (i.e., that can migrate landward during transgressions; e.g., Helland-Hansen et al., 2012; Jones et al., 2015); and (2) the shelf-slope structures, at continental-margins scale, of hundreds to thousands of meters high formed by long-term subsidence (Helland-Hansen et al., 2012; Jones et al., 2015; see Patruno et al. [2015c] for a recent review). Although the New Jersey "intermediate-scale" clinoforms could be referred to as "mid-shelf delta" (Porębski and Steel, 2006) or "shelf-edge" or "shelf-prism" clinoforms (Helland-Hansen and Gjelberg, 2012 ; Patruno et al., 2015c), they show a range of scales from the small "delta" scale of a few tens of meters to the large "shelf-prism" scale >100 m thick during their progressive growth (see below and, e.g., Figs. 5 and 7). Such different scales can be preserved on present-day margins with sufficient accommodation space, such as in the Mediterranean Sea (e.g., Rabineau et al., 2006, 2014). The "shelf-prism" clinoforms prograde and accrete basinward or remain fixed through time (Helland-Hansen and Hampson, 2009) at 10^4 to 10^6 yr time scales (Vanney and Stanley, 1983), but can hardly backstep.

The New Jersey clinothems sit on low-angle (<1°) Eocene carbonate ramp deposits controlled by differential subsidence that were starved of siliciclastic input until the late Oligocene (Steckler, 1999). Due to global climate cooling and the correlative increase in sediment supply, the clinoforms started to nucleate (by delta progradation) during the late Oligocene to early Miocene, progressively building up the present-day shelf margin. These clinoforms built by the progressive growth of small-scale prograding subaerial-subaqueous deltas merged into large-scale shelf-prism (*sensu* Patruno et al., 2015a) or shelf-edge (*sensu* Helland-Hansen and Hampson, 2009) clinoforms, building a compound clinoform (*sensu* Jones et al., 2015; Patruno et al., 2015a). This large-scale geometry is controlled by a number of parameters, including long-term subsidence, global sea-level changes, sediment supply, and oceanic currents, among others (e.g., Patruno et al., 2015a). The New Jersey clinoform complex sits on an initial topography that was three to five times steeper than the present-day shelf profile (1:300–1:500 slope versus 1:1000 at present) (Steckler et al., 1999). The height of the clinoform rose progressively in a concave-up ascending trajectory, from 26 m in seismic unit m6 to a maximum of 250 m in m4 (46 m in m5.6, 116 m in m5.4, 131 m in m5) (Steckler et al., 1999), with a quite constant flooding water depth of 60–120 m at the toe of the clinoform (Katz et al., 2013) except at m4, the discussion of which is beyond the scope of this paper.

Characteristically, this intrashelf clinoform complex is largely composed of muds with <~30% clean sands and coarse material transported at the rollover and beyond at the toe of the slope (see example and discussion in Poyatos-Moré et al. [2016]). The shelf (i.e., the clinothem topset) is storm-influenced mud where the slope comprises a mud wedge largely dominated by density current deposits (flood, low-density turbidites). Its architecture includes a composite stack of clinothem units (Fig. 7).

Sequence Stratigraphic Interpretation of the Clinothem Deposits

Individual Clinothem Units

The seismic (or clinothem) units, which correspond in cores to T-R depositional sequences, are composed of seismic sets, which correspond in cores to the following systems (facies) tracts: (1) seismic set 1 with amalgamated toe-of-slope debrites that drape the toe of the slope (lithofacies association FA 1.2); (2) seismic set 2 with low-angle progradational muds deposited at the clinothems topset (storm-influenced FA2.1b, FA2.2b); (3) seismic set 3 with flood- to storm-influenced offshore muds (FA2.1 and FA2.2) to shoreface silty sands

(FA3) building the foreset where debrites and slope apron deposits (FA1.2) drape the toe of slope; and (4) seismic set 4, which is largely shoreface sand (FA3, FA4), pebbles, and gravels and gully fills (FA5) expressed as high-angle progradational reflectors at, or just beyond, the clinothem rollover (Figs. 5, 6, 7, and 8).

Set 3 shows a composite set of progradational reflectors with a marked increase in reflector angle and progradational rate with respect to seismic set 2. Internal unconformities of limited lateral extent produced by lobe switching during avulsion correlate to parasequence boundaries in coreholes. Seismic set 4 is bounded above by a maximum regressive surface capped by transgressive ravinement deposits on the shelf. This maximum regressive surface has been correlated in several instances with seismic sequence boundaries recognized by reflector terminations (Monteverde et al., 2008; Mountain et al., 2010; Miller et al., 2013a, 2013b).

According to Catuneanu's (2006) sequence stratigraphy nomenclature, the suite of systems tracts could be interpreted in one of two ways: hypothesis 1 (forced regressive delta), in which a healing-phase transgressive systems tract (in set 1) is overlain by a composite package comprising a highstand systems tract (low-angle mud, set 2), a forced regressive wedge (high-angle, upper offshore to shoreface sand downlapping onto coarse slope apron, set 3), and a lowstand systems tract (coarse shoreface sands and gully fills, set 4); or alternatively, hypothesis 2 (highstand delta), in which a lowstand systems tract (toe-of-slope debrites in set 1) is overlain by a thick and composite highstand systems tract (offshore muds to shoreface sands in sets 2, 3, 4). In both interpretations, ravinement deposits at the top of the shelf and glauconitic condensed horizons at the toe of the slope correspond to the transgressive systems tract.

The first hypothesis ("forced regressive" delta) is supported by (1) the lateral change in reflector configurations from low-angle sigmoidal (progradational-aggradational) in highstand systems tract (set 2) due to the predominance of fine-grained lithologies (Patruno et al., 2015c) to sandier oblique (progradational) in forced regressive systems tract (set 3) and high-angle oblique in lowstand systems tract (set 4) building up the upper slope; (2) the lack of clear aggradational topsets at the clinothem unit scale; (3) the sharp angular surfaces at base of seismic sets 3 and 4; (4) the presence of a zone of separation and bypass (tens of kilometers large) between the shoreface sands at the rollover and subaerial delta at the shoreline; (5) the increasing average grain size in regressive deposits from proximal to distal settings, which implies an increasing winnowing of earlier highstand deposits; and (6) coarse-grained sedimentation on the slope apron at the base of set 3 (sequence boundary *sensu* Posamentier and Morris [2000]). The progressive increase in the angle of progradation together with the height of the foreset correspond to the lateral change from low angle subaqueous delta sedimentation during highstand time to the outbuilding of shelf-prism scale clinoforms during forced regressive and lowstand times.

The second hypothesis ("highstand" delta) is supported by (1) the overall progradational, i.e., normal regressional, seismic reflector configuration; (2) the lack of seaward downstepping subaerial erosion and incision at the rollover, indicative of a net sea-level fall; (3) the presence of offshore muds on the shelf instead of relics of shoreface-delta sands, which in the first hypothesis should bring the sand to the rollover; and (4) the lack of clear erosion surfaces in cores at the base of sets 3 (force regressive) and 4 (lowstand). In this "highstand hypothesis", the dip of the clinoform foresets precludes the preservation of lowstand shoreface sands, which are reworked in mass flows downslope beyond the rollover in the slope apron.

The New Jersey clinoforms follow a progradational, horizontal trajectory, with clinoforms as high as the mid-shelf water depth, with no paralic or coastal plain deposits, and a shelfal foreset underlined by turbidite deposits, which correspond to the main basic characters of mid-shelf deltas (Porębski and Steel, 2006). In such a context, the normal regressional shape of the clinoforms in seismic data does not necessarily mean that the bulk of the clinoforms was deposited during highstand to stillstand times of relative sea level. Indeed, shelf-prism clinoforms can only accrete basinward and then can remain fixed through time (Helland-Hansen and Hampson, 2009) over periods as long as 10^4 to 10^6 yr (Vanney and Stanley, 1983). They bathe in a maximum water depth of about the same magnitude as the height of the clinoforms before starvation. Sigmoidal morphologies in set 2 (in hypothesis 2, "highstand delta") are due to the predominance of fine-grained lithologies, the influence of basinal processes, the relatively slow progradation, and the high-angle trajectories (Porębski and Steel, 2006), as one can find in subaqueous deltas. With relative sea-level fall and the correlative increase in wave action on the shelf, sediments bypassing the shelf augment the sand content and sorting in the distal seaward-prograding increments (Sydow and Roberts, 1994; Anderson et al., 2004), producing basinward detached delta bodies generating the typical oblique profiles in sets 3 and 4 (in hypothesis 1, "forced regressive and lowstand deltas"), but no exposure of the shelf. The latter, at the difference of subaerial deltas, do not show important downcuttings during relative sea-level falls (Helland-Hansen and Hampson, 2009), and the unconformities can be quite remote (Porębski and Steel, 2006), but significant amounts of sand are delivered to the slope and the basin floor. After a major flooding, the shelf-prism clinoforms are separated from the highstand shoreline by a muddy shelf, but both can coincide when the shoreline delta transits across the shelf, giving rise to the so-called shelf-edge deltas (Porębski and Steel, 2003; Burgess et al., 2008; Helland-Hansen and Gjelberg, 2012). Transgressive as well as regressive wave ravinement can sharply truncate the shelf-prism clinoforms in wave-dominated coasts (15–40 m of erosion; Rodriguez et al., 2001; Bhattacharya and Willis, 2001; Cattaneo and Steel, 2002) as can geostrophic currents during early highstand (Rine et al., 1991).

The debate to determine whether the bulk of those shelf-prism clinoforms corresponds to highstand or forced regressive sediment bodies compares to the distinction made between supply-driven deltas (or "highstand deltas") and accommodation-driven deltas (or "forced regressive deltas") (Porębski and Steel, 2006). Supply-driven deltas (or "highstand deltas") show thick, stacked, sandy parasequences sets and extensive muddy low-energy delta front deposits damped in increasing water depths. Relative sea-level falls produce no incision at the shelf edge, and shelf-attached sandy delta fronts rather than a

basin-floor fan. Supply-driven deltas are very stable features where sequence boundaries (type 2 *sensu* Posamentier et al., 1988) can be unidentifiable at the base of shelf margin systems tracts. Accommodation-driven deltas (or "forced regressive deltas") show horizontal progradational rather than progradational-aggradational trajectories, no coastal plain deposits, and a proximal-distal increase in wave action transporting sands at the rollover. They are more unstable features with internal unconformities. Large-amplitude sea-level falls produce shelf-edge detached delta bodies that steepen the delta front when those shelf-edge deltas reach the deeper mid-shelf. These sea-level falls do not expose the shelf because the sediments that bypass the shelf-enhance the sand content in the more distal portion of the seaward progradational elements (Sydow and Roberts, 1994; Anderson et al., 2004). Both supply- and accommodation-driven deltas are truncated in the landward direction by wave and geostrophic-current ravinement, which control the preservation of topset-foreset deposits, and are overlain by open-shelf mudstones. New Jersey clinothems share more characteristics with accommodation-driven (forced regressive) deltas, but some clinoform progradational-aggradational trajectories, low-energy muddy clinoform foresets, and the lack of incision at the shelf edge are indicative of the influence of sediment supply in the overall architecture.

Stacks of Clinothem Units

The clinothem units are stacked in four large T-R sequences (stacks A–D, Fig. 7). Each T-R sequence comprises three to five clinothem units showing a period of backstepping followed by a progressive but marked seaward migration of the offlap break. This evolution is interpreted as the result of a rise followed by a fall in relative sea level. The landward-stepping clinothem units are sand rich, enriched with glauconite and thinner than seaward-stepping units. During the rise in sea level, the rollovers build out and then backstep, accumulating clean sands in wave-dominated shoreface deposits during late lowstand and transgressive times. On the shelf, the clinothem units are truncated by wave ravinement surfaces overlain by storm-influenced clayey silts that drape the flat shelf. This surface, which marks the transition from low-angle to flat-topped shelf style, is formed by wave-induced current erosion possibly linked to the successive seaward and landward shifts of the shoreline, attested by the presence of relics of wave-dominated sharp-based shoreface sand deposits at the rollover. The seaward-stepping clinothem units are thicker and show an overall increase in the sand-mud ratio through time and thinning out by erosion at the top. Each of them comprises a suite of well-developed sediment packages including, from the oldest to the youngest: (1) low-angle, sigmoidal to oblique progradation of muddy clinothems of subaqueous deltas (highstand time), bypassed by (2) high-angle, shelf-edge deltas with switching lobes, high terrestrial inputs, and flood-induced hyperpycnal flows (forced regression time) and (3) disconnected delta front sands that accumulate at the shelf edge (lowstand time). In contrast with the landward-stepping units, the last two packages of sediments are enriched with terrestrial material like micas and organic detritus. The large T-R sequences show thin backstepping patterns that appear contradictory with Helland-Hansen and Hampson's (2009) observations that shelf-scale clinoforms cannot backstep as the smaller-scale subaqueous deltas can do.

The New Jersey cross-section shows a progressive construction of the clinoform slope through time. Stack A is largely progradational. Individual sequences are strongly eroded, with just the lower part of their slopes preserved possibly due to higher-order forced regression. Stack B is progradational to aggradational, with a well-preserved sand-rich clinoform rollover. From this stack upward, the clinothems are taller (>250 m) and steeper (dip >2.5°), still migrating seaward drastically (>33 km laterally in stack D; Steckler et al., 1999). Large volumes of fine-grained material drape the clinoform front whose sediment differential compaction produced a depression at its toe moving in a seaward direction (rolling syncline effect of Steckler et al. [1999]).

A Depositional Model for the New Jersey Miocene Clinoforms

Core analysis and the reinterpretation of seismic line 529 show that a specific facies architecture, with mud-dominated deposits on the topset, foreset, and bottomset and sand-dominated facies at the rollover and the toeset, characterize the clinothems (Fig. 5). This spatial organization differs from that of predictive clinothem models (e.g., Catuneanu, 2006; Mountain et al., 2010b) and of previous studies based on seismic data alone (e.g., Poulsen et al., 1998; Monteverde et al., 2008). These models described a progressive increase in mud content in a seaward direction and a net accumulation of sand in the clinothem at the depositional shelf break.

ODP coreholes drilled on the New Jersey coastal plain record a stack of ~30-m-thick depositional sequences (Browning et al., 2008). The sequences display a basal muddy sandstone layer overlain by prodelta offshore marine muds giving rise upsection to delta front wave-dominated shoreface sands (Browning et al., 2008; Fig. 7). These successions are interpreted as amalgamated transgressive and highstand deposits of Miocene depositional sequences coeval with the clinothems drilled by IODP Expedition 313 coreholes 40–60 km in the offshore (Browning et al., 2008, 2013; Kominz et al., 2016). The falling stage and the lowstand deposits interpreted in the offshore are both missing in the onshore sequences.

Sediment Transport

The presence of mud-rich facies during highstand times on the topset of the clinoform on the shelf, between shoreface sand deposits at the rollover and sand-prone shoreline delta deposits 40–60 km landward, implies two possibilities: either (1) an important and rapid erosion that removed the entire uppermost sand-prone material on the topset of the clinoform after a 60+ km shoreface progradation and a shift of all of the facies belts to the depositional shelf

break (rollover) (e.g., Porębski and Steel, 2006), or (2) a compound depositional system that involves a subaerial delta that fed a distant subaqueous delta (e.g., Helland-Hansen and Hampson, 2009; Patruno et al., 2015) by current transportation. The first hypothesis requires the transit of deltas and shoreline bodies across the shelf during forced regression and lowstand times, providing sands to the rollover (Posamentier and Morris, 2000), with deltas being subsequently erased by transgressive ravinement (Porębski and Steel, 2006). The shelf is flattened twice by wave action during forced regression and transgression-early highstand. The second hypothesis requires significant near-bed shear stresses in shallow marine areas marked by high-energy waves, tides, or currents causing shelf flattening and bypass through lateral advection and resuspension of sediment (Pirmez et al., 1998; Driscoll and Karner, 1999; Swenson et al., 2005; Cattaneo et al., 2007; Patruno et al., 2015a; Poyatos-More et al., 2016). Deposition occurs preferentially seaward of the rollover where near-bed agitation decreases below the threshold of sediment motion (Mitchell, 2012; Mitchell et al., 2012). The latter hypothesis is well documented for subaqueous deltas, which are the prodelta counterparts of subaerial deltas. But, these compound bodies are small, at delta scale, a few meters to tens of meters high, and can step back and forth during transgression-regression processes, which is different from what we observe on the very stable New Jersey shelf-prism clinoforms. Although many aspects of the dynamic and geometries of the shelf-prism and delta-scale clinoforms are reputedly scale invariant (Patruno et al., 2015a), no clear sediment transport process is documented for sand transportation across the shelf by suspension and advection at the large-scale shelf-prism clinoforms. Moreover, the accommodation-driven cross-shelf transportation of sand postulated in the first hypothesis is attested by the relics of shoreface sands in the transgressive lags, the flatness of the shelf enhanced by the back-and-forth passage of the "wave base razor", a highstand water depth over 60 m beyond the fair-weather and storm wave base, and the presence of sharp surfaces at the base of the interpreted forced regressive and lowstand systems tracts indicative of drastic downward shifts of sediment. Nevertheless, it is very likely that both processes interact. A net fall in sea level, with a seaward migration of the shoreline delta and its subaqueous counterpart, would enhance near-bed shear stresses on the shelf, transporting sand to the rollover, without the strict necessity for the subaerial delta to prograde to the shelf edge. This mechanism would easily explain the lack of subaerial erosion (or deposition) in the corehole at the rollover and on the topset of clinoforms.

The Abundance of Mud

The New Jersey clinothems are made up of 70% muddy (clayey silt to silty clay) sediment mainly concentrated in highstand systems tracts, with sands being mostly concentrated at the rollover and at the toe of the slope. Shelfal muds result from the dispersal of river supply by dip-oriented current in high-sediment-supply conditions, or from alongshore currents settling contourite drifts in shallow waters (Hanebuth et al., 2015; Patruno et al., 2015a, 2015b, 2015c). Depending on sediment supply and tide and wave energy, mud dispersal on the shelf can form muddy clinothems detached from their subaerial counterparts ("subaqueous delta clinoforms", e.g., Fly River [Papua New Guinea] or Amazon River, in Walsh and Nittrouer, 2009) or shelf mud wedges ("marine dispersal dominated", e.g., Eel River [northern California, USA], in Walsh and Nittrouer, 2009). In the Holocene, shelf mud wedges seems mostly recorded in enclosed seas (e.g., Adriatic Sea: Trincardi, et al., 1994; Cattaneo et al., 2003; Yellow Sea and East China Sea: Liu et al., 2004, 2006), while deep water muddy clinothems are reported in open marine conditions, such as in the western and eastern Atlantic Ocean (Nittrouer et al., 1996; Hanebuth and Lantzsch, 2008; Hanebuth et al., 2015). Shelf mud wedges require a bathymetric low on the shelf to accumulate. An inner-shelf 6–12-m-scale low, deduced from backstripping, is thought to be the result of a dynamic topography effect (Kominz et al., 2016), but no wedging out of the seismic reflectors in a seaward direction on seismic sections substantiates this calculation, although it may be too small to be discriminated. The New Jersey clinoforms develop on a gently dipping shelf with a ramp-like morphology (apparent dip of 0.75°–0.5°; Miller et al., 2013a) bathed below mean storm wave base, in 30–50 m of water depth (e.g., Katz et al., 2013), 40–60 km seaward of the shoreline. This distance from the shoreline seems very likely because subaqueous delta clinoforms show higher accumulation rates than their subaerial counterparts and prograde three times further and faster than their contemporaneous shoreline (Patruno et al., 2015a). Such a separation is observed in the Holocene subaqueous deltas of the Amazon, with the rollover in ~80 m water depth, 10–100 km from the shoreline (Nittrouer et al., 1996; Walsh and Nittrouer, 2009), and in the ancient Blackhawk subaqueous delta (Santonian–Campanian [Utah]) sited in 50–80 m of water depth, 25–70 km from the paleocoastline (e.g., Hampson, 2010).

A Composite Scenario of Deposition

A composite scenario, comprising the interbedding of subaerial and subaqueous deltas and shelf-edge deltas, probably best represents the depositional model of the New Jersey clinoforms (Fig. 9). The subaerial delta and its muddy flood-influenced subaqueous delta prograde at low angle during normal regression of highstand time. During a net sea-level fall, the subaqueous delta is progressively overstepped by the subaerial delta. The increase of wave and storm currents and near-bed stresses on the shelf brings sand to the rollover, building shelf edge deltas (Dixon et al., 2012) in forced regressive and lowstand systems tracts of shelf-prism clinothems. During the subsequent rise in sea level, the rollover builds out and then backsteps, accumulating clean sands in wave-dominated shoreface deposits. The overlying transgressive deposits confirm that the shelf-edge delta deposits represent the lowstand system tract (shelf margin wedge type, above a type 2 sequence boundary *sensu* Posamentier et al. [1988]) not preserved in ODP onshore coreholes (Browning et al., 2008). On the shelf, the subaqueous deltas are truncated by wave ravinement surfaces overlain by storm-influenced clayey silts that drape a flattened shelf.

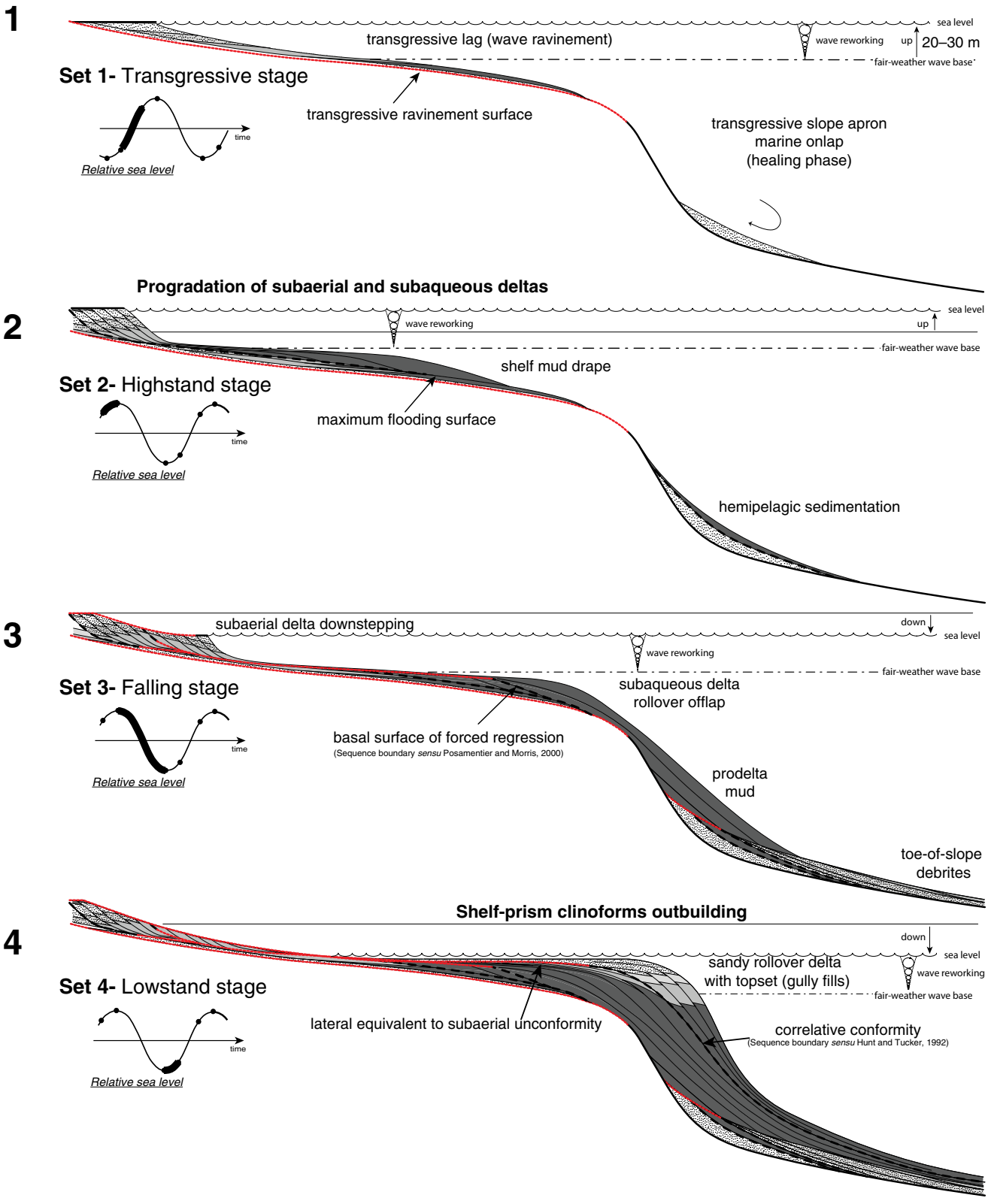

Figure 9 (*on this and following page*). Tentative conceptual model showing the relationships between relative sea-level change and the deposition of the lower to middle Miocene New Jersey shelf clinothems. This model is based on the R/V *Oceanus* cruise Oc270 seismic line 529 interpretations and core analysis retrieved in Holes M0027, M0028, and M0029. It shows the importance of rapid fall and rise of sea level on the disconnection of subaerial and subaqueous deltas on wide and flat shelves. ST—systems tracts.

Continued section with the next sets 1 (transgressive) and 2 (highstand)

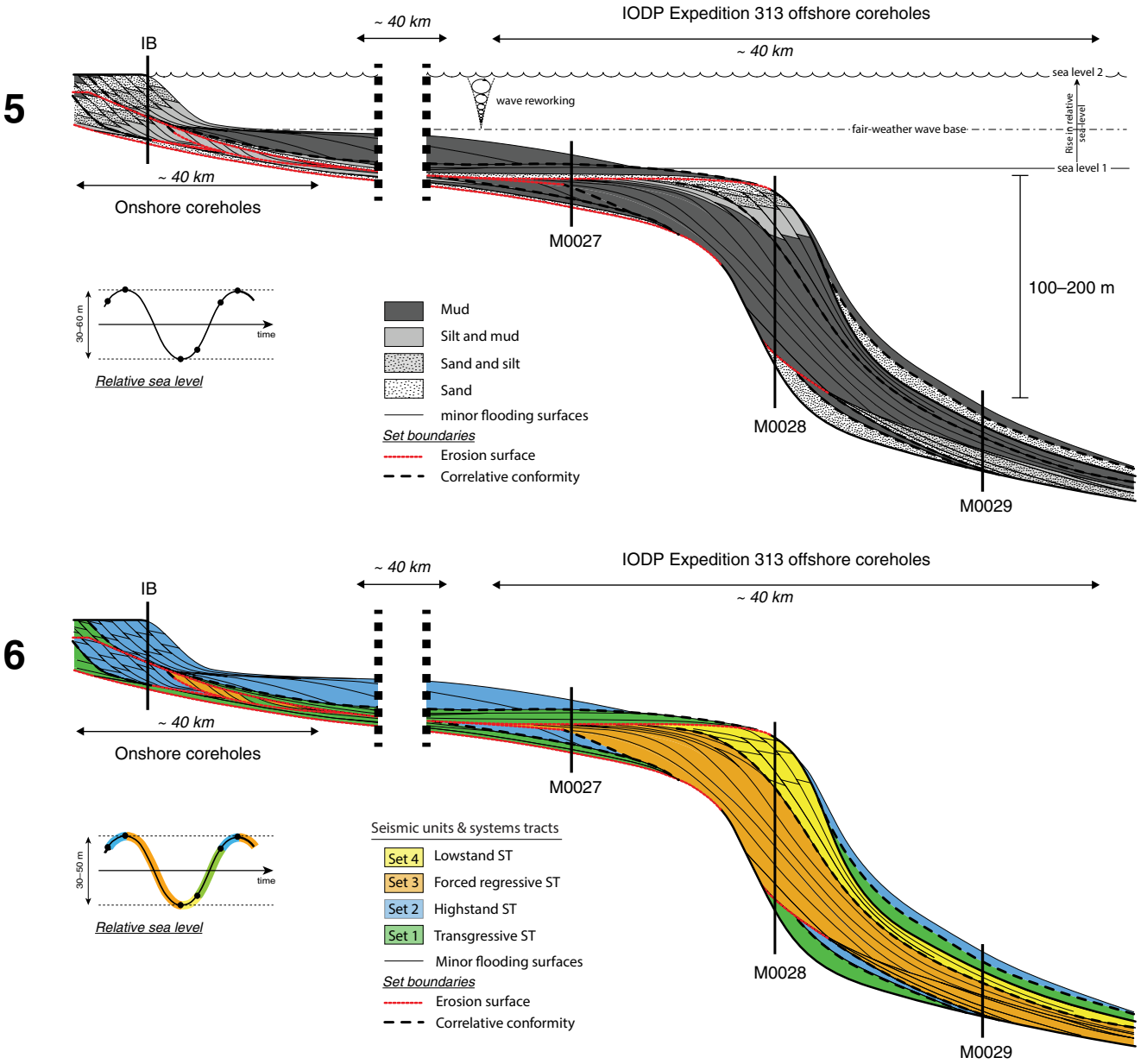

Figure 9 (*continued*).

Controls on Clinoform Architecture

Clinoforms are the basic building blocks of passive margin sedimentary architectures (e.g., Walsh et al., 2004; Helland-Hansen and Hampson, 2009; Patruno et al., 2015a). Their architecture is controlled by a number of forcing parameters that includes autocyclic (e.g., waves, currents, topography) and allocyclic (sea level, subsidence, sediment supply, and climate) controls.

The Clinoforms Record Changes in Accommodation Space

The New Jersey clinoforms as a whole show an overall concave-up ascending trajectory typical of a long-term relative sea-level rise compensated by a steady sediment supply filling space made available by eustasy and subsidence. The heights of the clinoforms increased progressively (26 m in sequence m6, to 46 m in sequence m5.6, 116 m in sequence m5.4, 131 m in m5, to a maximum of 250 m in sequence m4; Steckler et al., 1999) with a quite constant flooding water depth of 10 m to a few tens of meters. In detail, however, this architecture is composed of four stacks of clinothems, which are the consequences of marked differences in the response of the sedimentary system to changes in relative sea level (Figs. 7 and 9). Stack A is made up of low-gradient, sigmoidal, progradational, early Miocene clinoforms built by the wandering of subaqueous and shelf-edge delta lobes sharply truncated by an erosion surface during a net fall in relative sea level. Stack B is composed of oblique, progradational-aggradational, early middle Miocene clinoforms with well-preserved rollovers and clinoform slopes built during an overall rise in relative sea level. The clinothems comprise flat-top, low-gradient subaqueous delta lobes bypassed by wave-dominated, shoreface delta sands during forced regression due to the reduced accommodation space on the shelf (Fig. 9). The wave-dominated, shoreface delta sands accumulated with high-angle, oblique geometries, where space is available for sediment to accumulate, i.e., beyond the rollover. The combined action of (1) storm waves during highstand and fair-weather waves during forced regression and (2) the seaward shift of the shoreface toward the rollover (so-called regressive surface of marine erosion; e.g., Proust et al., 2001) shaped the flat surface at the top of the subaqueous delta. The shoreface sand and the subaqueous delta may be separated by tens of kilometers laterally and tens of meters vertically in water depth, depending on the intensity of wave and tide activity like that observed in the Ganges, Brahmaputra, Amazon, and Huang He (Yellow) river examples (Nittrouer et al. 1996; Kuehl et al., 1997; Michels et al., 1998; Hernández-Molina et al., 2000; Walsh et al., 2004; Patruno et al., 2015a, 2015c). From stack C upward (Fig. 7), the clinothems became definitively taller (>250 m) and steeper (>2.5°) and started migrating seaward at a faster pace. Large volumes of fine-grained sediment draped the slope during highstand times.

The Importance of a Flat Shelf (Clinoform Topset)

The progressive flattening of the New Jersey shelf during the Miocene increased the sedimentation rate along the clinoform foreset (cf. stacks B and C) feeding slope-apron and toe-of-slope fans (cf. stack A). This increased (1) the progradation rate of the shelf (3–5 km/m.y. in the early Miocene to 16–17 km/m.y. in the middle Miocene; Steckler et al., 1999; Carvajal et al., 2009), (2) the height of the slope (22–46 m in the early Miocene to 175–256 in the middle Miocene) and (3) the dip of the slope (1°–2.7°) of the clinoforms with almost no change in the highstand shelf water depth (30–75 m; Katz et al., 2013). Surprisingly, the New Jersey shelf-prism clinoforms do not show any indication of significant autoretreat (Helland Hansen et al., 2012) due to overextension and insufficient sediment supply, nor oversteepening and increasing water depth during the early Miocene to early mid-Miocene. These long-term rates of progradation are similar to those retained globally (10–500 km/m.y.; Patruno et al., 2015a), but the rate of progradation seems to have slowed down a little bit later (m4, 12.5 Ma; Steckler et al., 1999) probably due to oversteepening when the dip of the clinoforms reached 2.5°. With such a dip, 100 m of drop in sea level, which would have been unlikely, would have only produced 3 km of progradation (Burgess et al., 2008).

The Importance of Climate Change

The increase in the intensity of waves (height, recurrence intervals) favors the separation between subaqueous and subaerial deltas (Kuehl et al., 1997; Swenson et al., 2005), and as a consequence, the formation of a flat topset, the decrease in flood frequency and fluvial discharge, the overall progressive decrease in sediment grain size (from clinothem m5.45 onwards), as well as the increase in sedimentation rate on the slope of the subaqueous delta clinoforms. All of these are recognized as preliminary signals that might indicate the entry into the Neogene icehouse world (Helland Hansen et al., 2012). Large continental ice sheets grew and decayed in Antarctica in the early Miocene to early middle Miocene (Barrett et al., 1987; Miller et al., 1991; Zachos et al., 2001) (reduced ice sheets in the Northern Hemisphere at that time; Wolf-Welling et al., 1996; Wright and Miller, 1996) but stabilized with the installation of a permanent large continental ice sheet in East Antarctica at ca. 14.6–13.0 Ma (deep-sea Miocene isotope events Mi2a, Mi3, Mi4; Miller et al., 1991) during deposition of clinothems m5.2 to m4.1 (Browning et al., 2013). The later m4.1 corresponds to the onset of large-amplitude and low-frequency sea-level changes that resulted in the increasing rate of clinoform progradation.

CONCLUSION

Passive margins are considered as the places of simple, undeformed sedimentation that can be easily correlated over large distances, which theoretically offers the possibility of quantifying changes in global sea level. The clas-

sical depositional model is composed of prograding clinoforms well imaged at a large scale by seismic techniques. Their internal structure is rarely exposed or cored, although detailed knowledge of their architecture can definitively improve our understanding of their origin and the distribution pattern of geological reservoirs.

The New Jersey clinothem complex comprises mud with ~30% sand and coarse material concentrated at the rollover, the foreset, and the toe of the clinoform and beyond. Clinothems nucleate by delta progradation on topography three to five times steeper than the present-day shelf. Their compound depositional system involves a subaerial delta feeding a shelf-edge subaqueous delta lying on a gently deepening ramp-like morphology, typically set below fair-weather wave base. The low-angle foreset muds prograde during highstand times when subaerial shoreface sand and coarse material transit to the rollover and the toe of the clinoform during forced regression and lowstand times, where it accumulates in large shelf prism–scale clinothems. Sea level has never dropped below the rollover, but the back-and-forth displacements of the wave-base razor as well as the geostrophic current flatten the shelf and control the decoupling of the subaerial and subaqueous shelf-edge deltas.

The New Jersey clinothems show a curious example of the dynamic equilibrium between the geometry of the sediment body and control parameters (eustasy, subsidence, and sediment supply): the height of the clinoforms, the dip of the slope, and the progradation rate increase with no change in the water depth on the shelf, strictly controlled by the wave-base razor. The latter appears to be a first-order parameter controlling sediment progradation responsible for sediment transportation and bypass from the subaerial delta shoreline to the toe of the clinoforms, and, depending on sea-level and climate changes—climate cooling intensifies the wave regime—controls the overall geometry of the clinothems.

ACKNOWLEDGMENTS

This paper used samples and data provided by the Integrated Ocean Drilling Program (IODP) and the International Continental Scientific Drilling Program (ICDP). The research was supported by the CNRS-Institut National des Sciences de l'Univers 2010 Post-Campagne Research Program and a CNRS-IODP France postdoctoral grant A64622 to Hugo Pouderoux. We acknowledge funding from NERC (NE/F001428/1) to Hesselbo, and NERC (NE/H014306/1) to Hodgson. We are grateful to two anonymous reviewers for the careful review and editing of a previous version of this manuscript. This work has benefited from their valuable expertise and ideas. This paper is part of *Geosphere* themed issue Results of IODP Exp313: The History and Impact of Sea-Level Change Offshore New Jersey with guest associate editors G. Mountain, J.-N. Proust, and D.B. McInroy.

REFERENCES CITED

Alexander, C.R., Demaster, D.J., and Nittrouer, C.A., 1991, Sediment accumulation in a modern epicontinental-shelf setting: The Yellow Sea: Marine Geology, v. 98, p. 51–72, https://doi.org/10.1016/0025-3227(91)90035-3.

Anderson, J.B., Rodriguez, A., Abdulah, K.C., Fillon, R.H., Banfield, L.A., McKeon, H.A., and Wellner, J.S., 2004, Late Quaternary stratigraphic evolution of the northern Gulf of Mexico margin: A synthesis, *in* Anderson, J.B., and Fillon, R.H., eds., Late Quaternary Stratigraphic Evolution of the Northern Gulf of Mexico Margin: SEPM (Society for Sedimentary Geology) Special Publication 79, p. 1–23, https://doi.org/10.2110/pec.04.79.0001.

Ando, H., Oyama, M., and Nanayama, F., 2014, Data report: Grain size distribution in Miocene successions, IODP Expedition 313 Sites M0027, M0028, and M0029, New Jersey shallow shelf, *in* Mountain, G., Proust, J.-N., McInroy, D., Cotterill, C., and the Expedition 313 Scientists: Proceedings of the Integrated Ocean Drilling Program, Volume 313: Tokyo, Integrated Ocean Drilling Program Management International, Inc., 19 p., https://doi.org/10.2204/iodp.proc.313.201.2014.

Austin, J.A., Jr., Fulthorpe, C.S., Davies, C.A., and Lagoe, M.B., 1995, Unraveling the stratigraphic complexities of the last deglaciation: Ultra-high resolution 3D seismic images of the New Jersey continental shelf [abs.]: Eos (Transactions, American Geophysical Union), v. 76, Supplement, p. F308.

Austin, J.A., Jr., Fulthorpe, G.S., Mountain, G.S., Orange, D., and Field, M.E., 1996, Continental-margin seismic stratigraphy: Assessing the preservation potential of heterogeneous geologic processes operating on continental shelves and slopes: Oceanography (Washington, D.C.), v. 9, p. 173–177, https://doi.org/10.5670/oceanog.1996.06.

Barrett, P.J., Elston, D.P., Harwood, D.M., McKelvey, B.C., and Webb, P.N., 1987, Mid-Cenozoic record of glaciation and sea-level change on the margin of the Victoria Land basin, Antarctica: Geology, v. 15, p. 634–637, https://doi.org/10.1130/0091-7613(1987)15<634:MROGAS>2.0.CO;2.

Berg, O.R., 1982, Seismic detection and evaluation of delta and turbidite sequences: Their application to exploration for the subtle trap: American Association of Petroleum Geologists Bulletin, v. 66, p. 1271–1288.

Bhattacharya, J.P., and Willis, B.J., 2001, Lowstand deltas in the Frontier Formation, Powder River Basin, Wyoming: Implications for sequence stratigraphic models: American Association of Petroleum Geologists Bulletin, v. 85, p. 261–294, https://doi.org/10.1306/8626C7B7-173B-11D7-8645000102C1865D.

Browning, J.V., Miller, K.G., McLaughlin, P.P., Kominz, M.A., Sugarman, P.J., Monteverde, D., Feigenson, M.D., and Hernandez, J.C., 2006, Quantification of the effects of eustasy, subsidence, and sediment supply on Miocene sequences, mid-Atlantic margin of the United States: Geological Society of America Bulletin, v. 118, p. 567–588, https://doi.org/10.1130/B25551.1.

Browning, J.V., Miller, K.G., Sugarman, P.J., Kominz, M.A., McLaughlin, P.P., and Kulpecz, A.A., 2008, 100 Myr record of sequences, sedimentary facies and sea level change from Ocean Drilling Program onshore coreholes, US Mid-Atlantic coastal plain: Basin Research, v. 20, p. 227–248, https://doi.org/10.1111/j.1365-2117.2008.00360.x.

Browning, J.V., Miller, K.G., Sugarman, P.J., Barron, J., McCarthy, F.M.G., Kulhanek, D.K., Katz, M.E., and Feigenson, M.D., 2013, Chronology of Eocene–Miocene sequences on the New Jersey shallow shelf: Implications for regional, interregional, and global correlations: Geosphere, v. 9, p. 1434–1456, https://doi.org/10.1130/GES00857.1.

Burgess, P.M., Steel, R.J., and Granjeon, D., 2008, Stratigraphic forward modeling of basin-margin clinoform systems: Implications for controls on topset and shelf width and timing of formation of shelf-edge deltas, *in* Hampson, G.J., Steel, R.J., Burgess, P.M., and Dalrymple, R.W., eds., Recent Advances in Models of Siliciclastic Shallow-Marine Stratigraphy: SEPM (Society for Sedimentary Geology) Special Publication 90, p. 35–45, https://doi.org/10.2110/pec.08.90.0035.

Carvajal, C., Steel, R., and Petter, A., 2009, Sediment supply: The main driver of shelf-margin growth: Earth-Science Reviews, v. 96, p. 221–248, https://doi.org/10.1016/j.earscirev.2009.06.008.

Cattaneo, A., and Steel, R.J., 2002, Transgressive deposits: A review of their variability: Earth-Science Reviews, v. 62, p. 187–228, https://doi.org/10.1016/S0012-8252(02)00134-4.

Cattaneo, A., Correggiari, A., Penitenti, D., Trincardi, F., and Marsset, T., 2003, Morphobathymetry of small-scale mud reliefs on the Adriatic shelf, *in* Locart, J., and Mienert, J., eds., Submarine Mass Movements and Their Consequences: Advances in Natural and Technological Hazards Research: Netherlands, Springer, p. 401–408, https://doi.org/10.1007/978-94-010-0093-2_44.

Cattaneo, A., Trincardi, F., Asioli, A., and Correggiari, A., 2007, The Western Adriatic shelf clinoform: Energy-limited bottomset: Continental Shelf Research, v. 27, p. 506–525, https://doi.org/10.1016/j.csr.2006.11.013.

Catuneanu, O., 2006, Principles of Sequence Stratigraphy: Elsevier, Amsterdam, 375 p.

Catuneanu, O., Abreu, V., Bhattacharya, J.P., Blum, M.D., Dalrymple, R.W., Eriksson, P.G., Fielding, C.R., Fisher, W.L., Galloway, W.E., Gibling, M.R., Giles, K.A., Holbrook, J.M., Jordan, R., Kendall, C.G.St.C., Macurda, B., Martinsen, O.J., Miall, A.D., Neal, J.E., Nummedal, D., Pomar, L., Posamentier, H.W., Pratt, B.R., Sarg, J.F., Shanley, K.W., Steel, R.J., Strasser, A.,

Tucker, M.E., and Winker, C., 2009, Towards the standardization of sequence stratigraphy: Earth-Science Reviews, v. 92, p. 1–33, https://doi.org/10.1016/j.earscirev.2008.10.003.
Davies, T.A., Austin, J.A., Lagoa, M.B., and Milliman, J.D., 1992, Late Quaternary sedimentation off New Jersey: New results using 3-D seismic profiles and cores: Marine Geology, v. 108, p. 323–343, https://doi.org/10.1016/0025-3227(92)90203-T.
Dixon, J.F., Steel, R.J., and Olariu, C., 2012, Shelf-edge delta regime as a predictor of deep-water deposition: Journal of Sedimentary Research, v. 82, p. 681–687, https://doi.org/10.2110/jsr.2012.59.
Driscoll, N.W., and Karner, G.D., 1999, Three-dimensional quantitative modeling of clinoform development: Marine Geology, v. 154, p. 383–398, https://doi.org/10.1016/S0025-3227(98)00125-X.
Eberli, G.P., Swart, P.K., Malone, M.J., et al., 1997, Proceedings of Ocean Drilling Program, Initial Reports, Volume 166: College Station, Texas, Ocean Drilling Program, https://doi.org/10.2973/odp.proc.ir.166.1997.
Embry, A.F., 2009, Practical Sequence Stratigraphy: Canadian Society of Petroleum Geologists, http://www.geoafricasciences.org, 81 p.
Fulthorpe, C.S., and Austin, J.A., Jr., 1998, Anatomy of rapid margin progradation: Three-dimensional geometries of Miocene clinoforms, New Jersey margin: American Association of Petroleum Geologists Bulletin, v. 82, p. 251–273.
Fulthorpe, C.S., Austin, J.A., Jr., and Mountain, G.S., 1999, Buried fluvial channels off New Jersey: Did sea-level lowstands expose the entire shelf during the Miocene?: Geology, v. 27, p. 203–206, https://doi.org/10.1130/0091-7613(1999)027<0203:BFCONJ>2.3.CO;2.
Greenlee, S.M., and Moore, T.C., 1988, Recognition and interpretation of depositional sequences and calculation of sea-level changes from stratigraphic data—Offshore New Jersey and Alabama Tertiary, *in* Wilgus, C.K., Hastings, B.S., Posamentier, H., Van Wagoner, J.C., Ross, C.A., and Kendall, C.G.St.C., eds., Sea-Level Changes: An Integrated Approach: SEPM (Society for Sedimentary Geology) Special Publication 42, p. 329–353, https://doi.org/10.2110/pec.88.01.0329.
Grow, J.A., Mattick, R.E., and Schlee, J.S., 1979, Multichannel seismic depth sections and interval velocities over outer continental shelf and upper continental slope between Cape Hatteras and Cape Cod, *in* Watkins, J.S., Montadert, L., and Dickerson, P.W., eds., Geological and Geophysical Investigations of the Continental Margins: American Association of Petroleum Geologists Memoir 29, p. 65–83.
Hampson, G.J., 2010, Sediment dispersal and quantitative stratigraphic architecture across an ancient shelf: Sedimentology, v. 57, p. 96–141, https://doi.org/10.1111/j.1365-3091.2009.01093.x.
Hanebuth, T.J.J., and Lantzsch, H., 2008, A Late Quaternary sedimentary shelf system under hyperarid conditions: Unravelling climatic, oceanographic and sea-level controls (Golfe d'Arguin, Mauritania, NW Africa): Marine Geology, v. 256, p. 77–89, https://doi.org/10.1016/j.margeo.2008.10.001.
Hanebuth, T.J.J., Lantzsch, H., and Nizou, J., 2015, Mud depocenters on continental shelves—Appearance, initiation times, and growth dynamics: Geo-Marine Letters, v. 35, p. 487–503, https://doi.org/10.1007/s00367-015-0422-6.
Haq, B.U., Hardenbol, J., and Vail, P.R., 1987, Chronology of fluctuating sea levels since the Triassic: Science, v. 235, p. 1156–1167, https://doi.org/10.1126/science.235.4793.1156.
Heezen, B.C., Tharp, M., and Ewing, M., 1959, The Floors of the Oceans. I. The North Atlantic. Text to Accompany the Physiographic Diagram of the North Atlantic: Geological Society of America Special Paper 65, 122 p.
Helland-Hansen, W., and Gjelberg, H., 2012, Towards a hierarchical classification of clinoforms: Abstract presented at American Association of Petroleum Geologists Annual Convention and Exhibition, Long Beach, California, 22–25 April, Search and Discovery article 90142.
Helland-Hansen, W., and Hampson, C.J., 2009, Trajectory analysis: Concept and applications: Basin Research, v. 21, p. 454–483, https://doi.org/10.1111/j.1365-2117.2009.00425.x.
Helland-Hansen, W., Steel, R.J., and Somme, T.O., 2012, Shelf genesis revisited: Journal of Sedimentary Research, v. 82, p. 133–148, https://doi.org/10.2110/jsr.2012.15.
Henriksen, S., Hampson, G.J., Helland-Hansen, W., Johannessen, E.P., and Steel, R.J., 2009, Shelf edge and shoreline trajectories, a dynamic approach to stratigraphic analysis: Basin Research, v. 21, p. 445–453, https://doi.org/10.1111/j.1365-2117.2009.00432.x.
Hernández-Molina, F.J., Fernández-Salas, L.M., Lobo, F., Somoza, L., Díaz-del-Río, V., and Alveirinho Dias, J.M., 2000, The infralittoral prograding wedge. A new large-scale progradational sedimentary body in shallow marine environments: Geo-Marine Letters, v. 20, p. 109–117, https://doi.org/10.1007/s003670000040.
Hesselbo, S.P., and Huggett, J.M., 2001, Glaucony in ocean-margin sequence stratigraphy (Oligocene–Pliocene, offshore New Jersey, USA; ODP Leg 174A): Journal of Sedimentary Research, v. 71, p. 599–607, https://doi.org/10.1306/112800710599.
Hodgson, D.M., Browning, J.V., Miller, K.G., Hesselbo, S.P., Poyatos-Moré, M., Mountain, G.S., and Proust, J.-N., 2017, Sedimentology, stratigraphic context, and implications of Miocene intrashelf bottomset deposits, offshore New Jersey: Geosphere, v. 14, p. 95–114, https://doi.org/10.1130/GES01530.1.
Hubbard, S.M., Fildani, A., Romans, B.W., Covault, J.A., and McHargue, T.R., 2010, High-relief slope clinoform development: Insights from outcrop, Magallanes Basin, Chile: Journal of Sedimentary Research, v. 80, p. 357–375, https://doi.org/10.2110/jsr.2010.042.
Hunt, D., and Tucker, M.E., 1992, Stranded parasequences and the forced regressive wedge systems tract: deposition during base-level fall: Sedimentary Geology, v. 81, p. 1–9, https://doi.org/10.1016/0037-0738(92)90052-S.
Inwood, J., Lofi, J., Davies, S., Basile, C.H., Bjerrum, C., Mountain, G., Proust, J.-N., Otsuka, H., and Valppu, H., 2013, Statistical classification of log response as an indicator of facies variation during changes in sea level: Integrated Ocean Drilling Program Expedition 313: Geosphere, v. 9, p. 1025–1043, https://doi.org/10.1130/GES00913.1.
Jones, G.E.D., Hodgson, D.M., and Flint, S.S., 2015, Lateral variability in clinoform trajectory, process regime, and sediment dispersal patterns beyond the shelf-edge rollover in exhumed basin margin-scale clinothems: Basin Research, v. 27, p. 657–680, https://doi.org/10.1111/bre.12092.
Katz, M.E., Browning, J.V., Miller, K.G., Monteverde, D.H., Mountain, G.S., and Williams, R.H., 2013, Paleobathymetry and sequence stratigraphic interpretations from benthic foraminifera: Insights on New Jersey shelf architecture, IODP Expedition 313: Geosphere, v. 9, p. 1488–1513, https://doi.org/10.1130/GES00872.1.
Kominz, M.A., Miller, K.G., Browning, J.V., Katz, M.E., and Mountain, G.S., 2016, Miocene relative sea level on the New Jersey shallow continental shelf and coastal plain derived from one-dimensional backstripping: A case for both eustasy and epeirogeny: Geosphere, v. 12, p. 1437–1456, https://doi.org/10.1130/GES01241.1.
Kotthoff, U., Greenwood, D.R., McCarthy, F.M.G., Müller-Navarra, K., Prader, S., and Hesselbo, S.P., 2014, Late Eocene to middle Miocene (33 to 13 million years ago) vegetation and climate development on the North American Atlantic Coastal Plain (IODP Expedition 313, site M0027): Climate of the Past, v. 10, p. 1523–1539, https://doi.org/10.5194/cp-10-1523-2014.
Kuehl, S.A., Levy, B.M., Moore, W.S. and Allison, M.A., 1997, Subaqueous delta of the Ganges-Brahmaputra river system: Marine Geology, v. 144, p. 81–96, https://doi.org/10.1016/S0025-3227(97)00075-3.
Liu, J.P., Milliman, J.D., Gao, S., and Cheng, P., 2004, Holocene development of the Yellow River's subaqueous delta, North Yellow Sea: Marine Geology, v. 209, p. 45–67, https://doi.org/10.1016/j.margeo.2004.06.009.
Liu, J.P., Li, A.C., Xu, K.H., Velozzi, D.M., Yang, Z.S., Milliman, J.D., and DeMaster, D.J., 2006, Sedimentary features of the Yangtze River–derived along-shelf clinoform deposit in the East China Sea: Continental Shelf Research, v. 26, p. 2141–2156, https://doi.org/10.1016/j.csr.2006.07.013.
Lofi, J., Inwood, J., Proust, J.-N., Monteverde, D.H., Loggia, D., Basile, C., Otsuka, H., Hayashi, T., Stadler, S., Mottl, M.J., Fehr, A., and Pezard, P.A., 2013, Fresh-water and salt-water distribution in passive margin sediments: Insights from Integrated Ocean Drilling Program Expedition 313 on the New Jersey Margin: Geosphere, v. 9, p. 1009–1024, https://doi.org/10.1130/GES00855.1.
McCarthy, F.M.G., Katz, M.E., Kotthoff, U., Browning, J.V., Miller, K.G., Zanatta, R., Williams, R.H., Drljepan, M., Hesselbo, S.P., Bjerrum, C.J., and Mountain, G.S., 2013, Sea-level control of New Jersey margin architecture: Palynological evidence from Integrated Ocean Drilling Program Expedition 313: Geosphere, v. 9, p. 1457–1487, https://doi.org/10.1130/GES00853.1.
Michels, K.H., Kudrass, H.R., Hübscher, C., Suckow, A., and Wiedicke, M., 1998, The submarine delta of the Ganges-Bramaputra: Cyclone-dominated sedimentation patterns: Marine Geology, v. 149, p. 133–154, https://doi.org/10.1016/S0025-3227(98)00021-8.
Miller, K.G., and Snyder, S.W., eds., 1997, Proceedings of the Ocean Drilling Program, Scientific Results, Volume 150X: College Station, Texas, Ocean Drilling Program, 374 p., https://doi.org/10.2973/odp.proc.sr.150x.1997.
Miller, K.G., Wright, J.D., and Fairbanks, R.G., 1991, Unlocking the Ice House: Oligocene–Miocene oxygen isotopes, eustasy, and margin erosion: Journal of Geophysical Research, v. 96, p. 6829–6848, https://doi.org/10.1029/90JB02015.

Miller, K.G., Mountain, G.S., Browning, J.V., Kominz, M., Sugarman, P.J., Christie-Blick, N., Katz, M.E., and Wright, J.D., 1998, Cenozoic global sea level, sequences, and the New Jersey Transect: Results from coastal plain and slope drilling: Reviews of Geophysics, v. 36, p. 569–601, https://doi.org/10.1029/98RG01624.

Miller, K.G., Kominz, M.A., and Browning, J.V., 2005, The Phanerozoic record of global sea-level change: Science, v. 310, p. 1293–1298, https://doi.org/10.1126/science.1116412.

Miller, K.G., Mountain, G.S., Browning, J.V., Katz, M.E., Monteverde, D., Sugarman, P.J., Ando, H., Bassetti, M.A., Bjerrum, C.J., Hodgson, D., Hesselbo, S., Karakaya, S., Proust, J.-N., and Rabineau, M., 2013a, Testing sequence stratigraphic models by drilling Miocene foresets on the New Jersey shallow shelf: Geosphere, v. 9, p. 1236–1256, https://doi.org/10.1130/GES00884.1.

Miller, K.G., Browning, J.V., Mountain, G.S., Bassetti, M.A., Monteverde, D., Katz, M.E., Inwood, J., Lofi, J., and Proust, J.-N., 2013b, Sequence boundaries are impedance contrasts: Coreseismic-log integration of Oligocene–Miocene sequences, New Jersey shallow shelf: Geosphere, v. 9, p. 1257–1285, https://doi.org/10.1130/GES00858.1.

Miller, K.G., Lombardi, C.J., Browning, J.V., Schmelz, W.J., Gallegos, G., Mountain, G.S., and Baldwin K.E., 2018, Back to basics of sequence stratigraphy: early Miocene and mid-Cretaceous examples from the New Jersey paleoshelf: Journal of Sedimentary Research, 2018, v. 88, p. 148–176, https://doi.org/10.2110/jsr.2017.73.

Mitchell, N.C., 2012, Modeling the rollovers of sandy clinoforms from the gravity effect on wave-agitated sand: Journal of Sedimentary Research, v. 82, p. 464–468, https://doi.org/10.2110/jsr.2012.48.

Mitchell, N.C., Masselink, G.D., Huthnance, J.M., Fernandez-Salas, L.M., and Lobo, F.J., 2012, Depths of modern coastal sand clinoforms: Journal of Sedimentary Research, v. 82, p. 469–481, https://doi.org/10.2110/jsr.2012.40.

Mitchum, R.M., Jr., Vail, P.R., and Sangree, J.B., 1977, Stratigraphic interpretation of seismic reflection patterns in depositional sequences, *in* Payton, C.E., ed., Seismic Stratigraphy—Applications to Hydrocarbon Exploration: American Association of Petroleum Geologists Memoir 26, p. 117–134.

Monteverde, D.H., Mountain, G.S., and Miller, K.G., 2008, Early Miocene sequence development across the New Jersey margin: Basin Research, v. 20, p. 249–267, https://doi.org/10.1111/j.1365-2117.2008.00351.x.

Mountain, G.S., Proust, J.-N., and McInroy, D., 2009, New Jersey shallow shelf: Shallow-water drilling of the New Jersey continental shelf: Global sea level and architecture of passive margin sediments: Integrated Ocean Drilling Program Scientific Prospectuses, v. 313, https://doi.org/10.2204/iodp.sp.313.2009.

Mountain, G., Proust, J.-N., and the Expedition 313 Science Party, 2010a, The New Jersey margin scientific drilling project (IODP Expedition 313): Untangling the record of global and local sea-level changes: Scientific Drilling, v. 10, p. 26–34, https://doi.org/10.5194/sd-10-26-2010.

Mountain, G., Proust, J.-N., McInroy, D., Cotteril, C., and the Expedition 313 Scientists, 2010b, Initial report: Proceedings of the International Ocean Drilling Program, Expedition 313: College Station, Texas, Ocean Drilling Program, http://publications.iodp.org/proceedings/313/313title.htm.

Neal, J., and Abreu, V., 2009, Sequence stratigraphy hierarchy and the accommodation succession method: Geology, v. 37, p. 779–782, https://doi.org/10.1130/G25722A.1.

Nittrouer C.A., Kuelh, S.A., Figueiredo, A.G., Allison, M.A., Sommerfield, C.K., Rine, J.M., Faria, L.E.C., and Silveira, O.M., 1996, The geological record preserved by Amazon shelf sedimentation: Continental Shelf Research, v. 16, p. 817–841, https://doi.org/10.1016/0278-4343(95)00053-4.

Patruno, S., Hampson, G.J., and Jackson, C.A.-L., 2015a, Quantitative characterisation of deltaic and subaqueous clinoforms: Earth-Science Reviews, v. 142, p. 79–119, https://doi.org/10.1016/j.earscirev.2015.01.004.

Patruno, S., Hampson, G.J., Jackson, C.A.-L., and Dreyer, T., 2015b, Clinoform geometry, geomorphology, facies character and stratigraphic architecture of a sand-rich subaqueous delta: Jurassic Sognefjord Formation, offshore Norway: Sedimentology, v. 62, p. 350–388, https://doi.org/10.1111/sed.12153.

Patruno, S., Hampson, G.J., Jackson, C.A.-L., and Whipp, P.S., 2015c, Quantitative progradation dynamics and stratigraphic architecture of ancient shallow-marine clinoform sets: A new method and its application to the upper Jurassic Sognefjord Formation, Troll Field, offshore Norway: Basin Research, v. 27, p. 412–452, https://doi.org/10.1111/bre.12081.

Pirmez, C., Pratson, L.F., and Steckler, M.S., 1998, Clinoform development by advection-diffusion of suspended sediment: Modeling and comparison to natural systems: Journal of Geophysical Research, v. 103, p. 24,141–24,157, https://doi.org/10.1029/98JB01516.

Poag, C.W., 1985a, Depositional history and stratigraphic reference section for central Baltimore Canyon trough, *in* Poag, C.W., ed., Geologic Evolution of the United States Atlantic Margin: New York, Van Nostrand Reinhold, p. 217–264.

Poag, C.W., 1985b, Cenozoic and Upper Cretaceous sedimentary facies and depositional systems of the New Jersey slope and rise, *in* Poag, C.W., ed., Geologic Evolution of the United States Atlantic Margin: New York, Van Nostrand Reinhold, p. 343–365.

Poag, C.W., 1992, U.S. middle Atlantic continental rise provenance, dispersal and deposition of Jurassic to Quaternary sediments, *in* Poag, C.W., and de Graciansky, P.C., eds., Geologic Evolution of Atlantic Continental Rises: New York, Van Nostrand Reinhold, p. 100–156.

Poag, C.W., and Schlee, J.S., 1984, Depositional sequences and stratigraphic gaps on submerged United States Atlantic margin, *in* Schlee, J.S., ed., Interregional Unconformities and Hydrocarbon Accumulation: American Association of Petroleum Geologists Memoir 36, p. 165–182.

Poag, C.W., and Sevon, W.D., 1989, A record of Appalachian denudation in postrift Mesozoic and Cenozoic sedimentary deposits of the U.S. middle Atlantic continental margin: Geomorphology, v. 2, p. 119–157, https://doi.org/10.1016/0169-555X(89)90009-3.

Poag, C.W., and Ward, L.W., 1987, Cenozoic unconformities and depositional supersequences of North Atlantic continental margins: Testing the Vail method: Geology, v. 15, p. 159–162, https://doi.org/10.1130/0091-7613(1987)15<159:CUADSO>2.0.CO;2.

Poag, C.W., and Ward, L.W., 1993, Allostratigraphy of the U.S. middle Atlantic continental margin—Characteristics, distribution, and depositional history of principal unconformity-bounded Upper Cretaceous and Cenozoic sedimentary units: U.S. Geological Survey Professional Paper 1542, 81 p.

Porębski, S.J., and Steel, R.J., 2003, Shelf-margin deltas: Their stratigraphic significance and relation to deep-water sands: Earth-Science Reviews, v. 62, p. 283–326, https://doi.org/10.1016/S0012-8252(02)00161-7.

Porębski, S.J., and Steel, R.J., 2006, Deltas and sea-level change: Journal of Sedimentary Research, v. 76, p. 390–403, https://doi.org/10.2110/jsr.2006.034.

Posamentier, H.W., and Morris, W.R., 2000, Aspects of the stratal architecture of forced regressive deposits, *in* Hunt, D., and Gawthorpe, R.L., eds., Sedimentary Responses to Forced Regressions: Geological Society of London Special Publication 172, p. 19–46, https://doi.org/10.1144/GSL.SP.2000.172.01.02.

Posamentier, H.W., Jervey, M.T., and Vail, P.R., 1988, Eustatic controls on clastic deposition I—Conceptual framework, *in* Wilgus, C.K., Hastings, B.S., Kendall, C.G.St.C., Posamentier, H.W., Ross C.A., and Van Wagoner, J.C., eds., Sea Level Changes: An Integrated Approach: Society of Economic Paleontologists and Mineralogists Special Publication 42, p. 109–124, https://doi.org/10.2110/pec.88.01.0109.

Poulsen, C.J., Flemings, P.B., Robinson, R.A.J., and Metzger, J.M., 1998, Three-dimensional stratigraphic evolution of the Miocene Baltimore Canyon region: Implications for eustatic interpretations and the systems tract model: Geological Society of America Bulletin, v. 110, p. 1105–1122, https://doi.org/10.1130/0016-7606(1998)110<1105:TDSEOT>2.3.CO;2.

Poyatos-Moré, M., Jones, G.D., Brunt, R.L., Hodgson, D.M., Wild, R.J., and Flint, S.S., 2016, Mud-dominated basin margin progradation: Processes and implications: Journal of Sedimentary Research, v. 86, p. 863–878, https://doi.org/10.2110/jsr.2016.57.

Proust, J.-N., Mahieux, G., and Tessier, B., 2001, Field and seismic images of sharp-based shoreface deposits: Implications for sequence stratigraphic analysis: Journal of Sedimentary Research, v. 71, p. 944–957, https://doi.org/10.1306/041601710944.

Rabineau, M., Berné, S., Olivet, J.-L., Aslanian, D., Guillocheau, F., and Joseph, P., 2006, Paleo sea levels reconsidered from direct observation of paleoshoreline position during Glacial Maxima (for the last 500,000 yr): Earth and Planetary Science Letters, v. 252, p. 119–137, https://doi.org/10.1016/j.epsl.2006.09.033.

Rabineau, M., Leroux, E., Aslanian, D., Bache, F., Gorini, C., Moulin, M., Molliex, S., Droz, L., dos Reis, A.T., Rubino, J.L., Guillocheau, F., and Olivet, J.L., 2014, Quantifying subsidence and isostatic readjustment using sedimentary paleomarkers, example from the Gulf of Lion: Earth and Planetary Science Letters, v. 388, p. 353–366, https://doi.org/10.1016/j.epsl.2013.11.059.

Reynolds, D.J., Steckler, M.S., and Coakley, B.J., 1991, The role of the sediment load in sequence stratigraphy: The influence of flexural isostasy and compaction: Journal of Geophysical Research, v. 96, p. 6931–6949, https://doi.org/10.1029/90JB01914.

Rine, J.M., Tillman, R.W., Culver, S.J., and Swift, D.J.P., 1991, Generation of late Holocene sand ridges on the middle continental shelf of New Jersey, U.S.A.—Evidence for formation in a mid-shelf setting based on comparison with nearshore ridge, *in* Swift, D.J.P., Oertel, G.F., Tillman, R.W., and Thorne, J.A., eds., Shelf Sand and Sandstone Bodies: International Association of Sedimentologists Special Publication 14, p. 395–423.

Rodriguez, A.B., Fassell, M.L., and Anderson, J.B., 2001, Variations in shoreface progradation and ravinement along the Texas coast, Gulf of Mexico: Sedimentology, v. 48, p. 837–853, https://doi.org/10.1046/j.1365-3091.2001.00390.x.

Schlee, J.S., 1981, Seismic stratigraphy of the Baltimore Canyon Trough: American Association of Petroleum Geologists Bulletin, v. 65, p. 26–53.

Sheridan, R.E., and Grow, J.A., eds., 1988, The Atlantic Continental Margin, U.S.: Boulder, Colorado, Geological Society of America, The Geology of North America, v. I-2, 610 p.

Steckler, M.S., Mountain, G.S., Miller, K.G., and Christie-Blick, N., 1999, Reconstruction of Tertiary progradation and clinoform development on the New Jersey passive margin by 2-D backstripping: Marine Geology, v. 154, p. 399–420, https://doi.org/10.1016/S0025-3227(98)00126-1.

Stevenson, C.J., Jackson, C.A.L., Hodgson, D.M., Hubbard, S.M., and Eggenhuisen, J.T., 2015, Deep-water sediment bypass: Journal of Sedimentary Research, v. 85, p.1058–1081, https://doi.org/10.2110/jsr.2015.63.

Swenson, J.B., Paola, C., Pratson, L., Voller, V.R., and Murray, A.B., 2005, Fluvial and marine controls on combined subaerial and subaqueous delta progradation: Morphodynamic modeling of compound-clinoform development: Journal of Geophysical Research, v. 110, F02013, https://doi.org/10.1029/2004JF000265.

Sydow, J., and Roberts, H.H., 1994, Stratigraphic framework of a late Pleistocene shelf-edge delta, northeast Gulf of Mexico: American Association of Petroleum Geologists Bulletin, v. 78, p. 1276–1312.

Trincardi, F., Correggiari, A., and Roveri, M., 1994, Late Quaternary transgressive erosion and deposition in a modern epicontinental shelf: The Adriatic semienclosed basin: Geo-Marine Letters, v. 14, p. 41–51, https://doi.org/10.1007/BF01204470.

Vail, P.R., and Mitchum, R.M., Jr., 1977, Seismic stratigraphy and global changes of sea level, Part 1: Overview, *in* Payton, C.E., ed., Seismic Stratigraphy: Applications to Hydrocarbon Exploration: American Association of Petroleum Geologists Memoir 26, p. 51–52.

Vail, P.R., Mitchum, R.M., Jr., Todd, R.G., Widmier, J.M., Thompson, S., III, Sangree, J.B., Bubb, J.N., and Hatlelid, W.G., 1977, Seismic stratigraphy and global changes of sea level, *in* Payton, C.E., ed., Seismic Stratigraphy: Applications to Hydrocarbon Exploration: American Association of Petroleum Geologists Memoir 26, p. 49–212.

Vanney, J.R., and Stanley, D.J., 1983, Shelfbreak physiography: An overview, *in* Stanley, D.J., and Moore, G.T., eds., The Shelf Break: Critical Interface on Continental Margins: Society of Economic Paleontologists and Mineralogists Special Publication 33, p. 1–24.

Van Sickel, W.A., Kominz, M.A., Miller, K.G., and Browning, J.V., 2004, Late Cretaceous and Cenozoic sea-level estimates: Backstripping analysis of borehole data, onshore New Jersey: Basin Research, v. 16, p. 451–465, https://doi.org/10.1111/j.1365-2117.2004.00242.x.

Van Wagoner, J.C., Mitchum, R.M., Campion, K.M., and Rahmanian, K.M., 1990, Siliciclastic Sequence Stratigraphy in Well Logs, Cores, and Outcrops: Concepts for High-Resolution Correlation of Time and Facies: American Association of Petroleum Geologists Methods in Exploration 7, 55 p.

Walsh, J.P., and Nittrouer, C.A., 2009, Understanding fine-grained river-sediment dispersal on continental margins: Marine Geology, v. 263, p. 34–45, https://doi.org/10.1016/j.margeo.2009.03.016.

Walsh, J.P., Nittrouer, C.A., Palinkas, C.M., Ogstaon, A.S., Sternberg, R.W., and Brunskill, G.J., 2004, Clinoform mechanics in the Gulf of Papua, New Guinea: Continental Shelf Research, v. 24, p. 2487–2510, https://doi.org/10.1016/j.csr.2004.07.019.

Watts, A.B., and Steckler, M.S., 1979, Subsidence and eustasy at the continental margin of eastern North America, *in* Talwani, M., Hay, W., and Ryan, W.B.F., eds., Deep Drilling Results in the Atlantic Ocean: Continental Margins and Paleoenvironment: American Geophysical Union Maurice Ewing Series 3, p. 218–234.

Withjack, M.O., Schlische, R.W., and Olsen, P.E., 1998, Diachronous rifting, drifting, and inversion on the passive margin of central eastern North America: An analog for other passive margins: American Association of Petroleum Geologists Bulletin, v. 82, p. 817–835.

Wolf-Welling, T.C.W., Cremer, M., O'Connell, S., Winkler, A., and Thiede, J., 1996, Cenozoic Arctic Gateway paleoclimate variability: Indications by changes in coarse-fraction composition (ODP Leg 151), *in* Thiede, J., Myhre, A.M., Firth, J.V., Johnson, G.L., and Ruddiman, W., eds., Proceedings of the Ocean Drilling Program, Scientific Results 151: College Station, Texas, Ocean Drilling Project) p. 515–525.

Wright, J.D., and Miller, K.G., 1996, Control of North Atlantic deep water circulation by the Greenland-Scotland Ridge: Paleoceanography, v. 11, p. 157–170, https://doi.org/10.1029/95PA03696.

Zachos, J.C., Shackleton, N.J., Revenaugh, J.S., Pälike, H., and Flower, B.P., 2001, Climate response to orbital forcing across the Oligocene-Miocene boundary: Science, v. 292, p. 274–278, https://doi.org/10.1126/science.1058288.